Journal of Controlled Release 328 (2020) 970–984

Contents lists available at ScienceDirect

Journal of Controlled Release

journal homepage: www.elsevier.com/locate/jconrel

Biotin-decorated all-HPMA polymeric micelles for paclitaxel delivery

Yan Wang[a], Mies J. van Steenbergen[a], Nataliia Beztsinna[a], Yang Shi[b], Twan Lammers[b], Cornelus F. van Nostrum[a], Wim E. Hennink[a,*]

[a] Department of Pharmaceutics, Utrecht Institute for Pharmaceutical Sciences, Utrecht University, Universiteitsweg 99, 3508 TB Utrecht, the Netherlands
[b] Department of Nanomedicine and Theranostics, Institute for Experimental Molecular Imaging, RWTH Aachen University Clinic, Forckenbecktrasse 55, 52074 Aachen, Germany

ARTICLE INFO

Keywords:
Polymeric micelles
N-2-Hydroxypropyl methacrylamide
Biotin
Drug targeting
Nanomedicines

ABSTRACT

To avoid poly(ethylene glycol)-related issues of nanomedicines such as accelerated blood clearance, fully *N*-2-hydroxypropyl methacrylamide (HPMAm)-based polymeric micelles decorated with biotin for drug delivery were designed. To this end, a biotin-functionalized chain transfer agent (CTA), 4-cyano-4-[(dodecylsulfanylthiocarbonyl)-sulfanyl]pentanoic acid (biotin-CDTPA), was synthesized for reversible addition–fragmentation chain-transfer (RAFT) polymerization. Amphiphilic poly(*N*-2-hydroxypropyl methacrylamide)-*block*-poly(*N*-2-benzoyloxypropyl methacrylamide) (p(HPMAm)-b-p(HPMAm-Bz)) with molecular weights ranging from 8 to 24 kDa were synthesized using CDTPA or biotin-CDTPA as CTA and 2,2′-azobis(2-methylpropionitrile) as initiator. The copolymers self-assembled in aqueous media into micelles with sizes of 40–90 nm which positively correlated to the chain length of the hydrophobic block in the polymers, whereas the critical micelle concentrations decreased with increasing hydrophobic block length. The polymer with a molecular weight of 22.1 kDa was used to prepare paclitaxel-loaded micelles which had sizes between 61 and 70 nm, and a maximum loading capacity of around 10 wt%. A549 lung cancer cells overexpressing the biotin receptor, internalized the biotin-decorated micelles more efficiently than non-targeted micelles, while very low internalization of both types of micelles by HEK293 human embryonic kidney cells lacking the biotin receptor was observed. As a consequence, the paclitaxel-loaded micelles with biotin decoration exhibited stronger cytotoxicity in A549 cells than non-targeted micelles. Overall, a synthetic pathway to obtain actively targeted poly(ethylene glycol)-free micelles fully based on a poly(HPMAm) backbone was established. These polymeric micelles are promising systems for the delivery of hydrophobic anticancer drugs.

1. Introduction

During the last decades, drug delivery systems have been extensively investigated for cancer chemotherapy, and particularly, substantial attention has been devoted to polymeric micelles [1–5]. Polymeric micelles are nanosized colloidal particles with a core-shell structure, which spontaneously self-assemble from amphiphilic copolymers above a certain concentration (CMC, critical micelle concentration) in aqueous solution. The outer hydrophilic shell ensures colloidal stability of polymeric micelles and provides long circulation in the blood circulation, whereas the hydrophobic core is highly suitable for accommodating and solubilizing hydrophobic drugs [6–9]. Due to their small size (< 100 nm) and long circulation kinetics, polymeric micelles passively accumulate in cancerous or inflamed tissues by a phenomenon referred to as the enhanced permeability and retention (EPR) effect [10–12]. Besides passive targeting, micelles can be functionalized with ligands for active targeting to increase the efficacy of anti-cancer drugs while reducing their unwanted localization in healthy tissues by means of receptor-mediated endocytosis [13–15]. Various ligands, including antibody (fragments), peptides, aptamers and small molecules (such as folate) have been employed for the design of targeted nanomedicines [16–19].

Biotin, as a water-soluble vitamin, is essential for normal cellular functions, growth and development [20,21], and the sodium-dependent multivitamin transporter (SMVT) has been proved to be its main transporter [22], which is overexpressed in many cancer cells such as lung cancer cells (A549 and M109) [20,23]. In 2004 Russell-Jones et al. reported that a biotin-targeted doxorubicin-poly(*N*-2-benzoyloxypropyl methacrylamide) (pHPMAm) conjugate caused significant killing enhancement in colon carcinoma xenografts. Importantly, the same

* Corresponding author.
E-mail addresses: y.wang3@uu.nl (Y. Wang), M.J.vanSteenbergen@uu.nl (M.J. van Steenbergen), nataliia.beztsinna@gmail.com (N. Beztsinna), yshi@ukaachen.de (Y. Shi), tlammers@ukaachen.de (T. Lammers), C.F.vanNostrum@uu.nl (C.F. van Nostrum), W.E.Hennink@uu.nl (W.E. Hennink).

https://doi.org/10.1016/j.jconrel.2020.09.013
Received 21 June 2020; Received in revised form 21 August 2020; Accepted 7 September 2020
Available online 12 September 2020

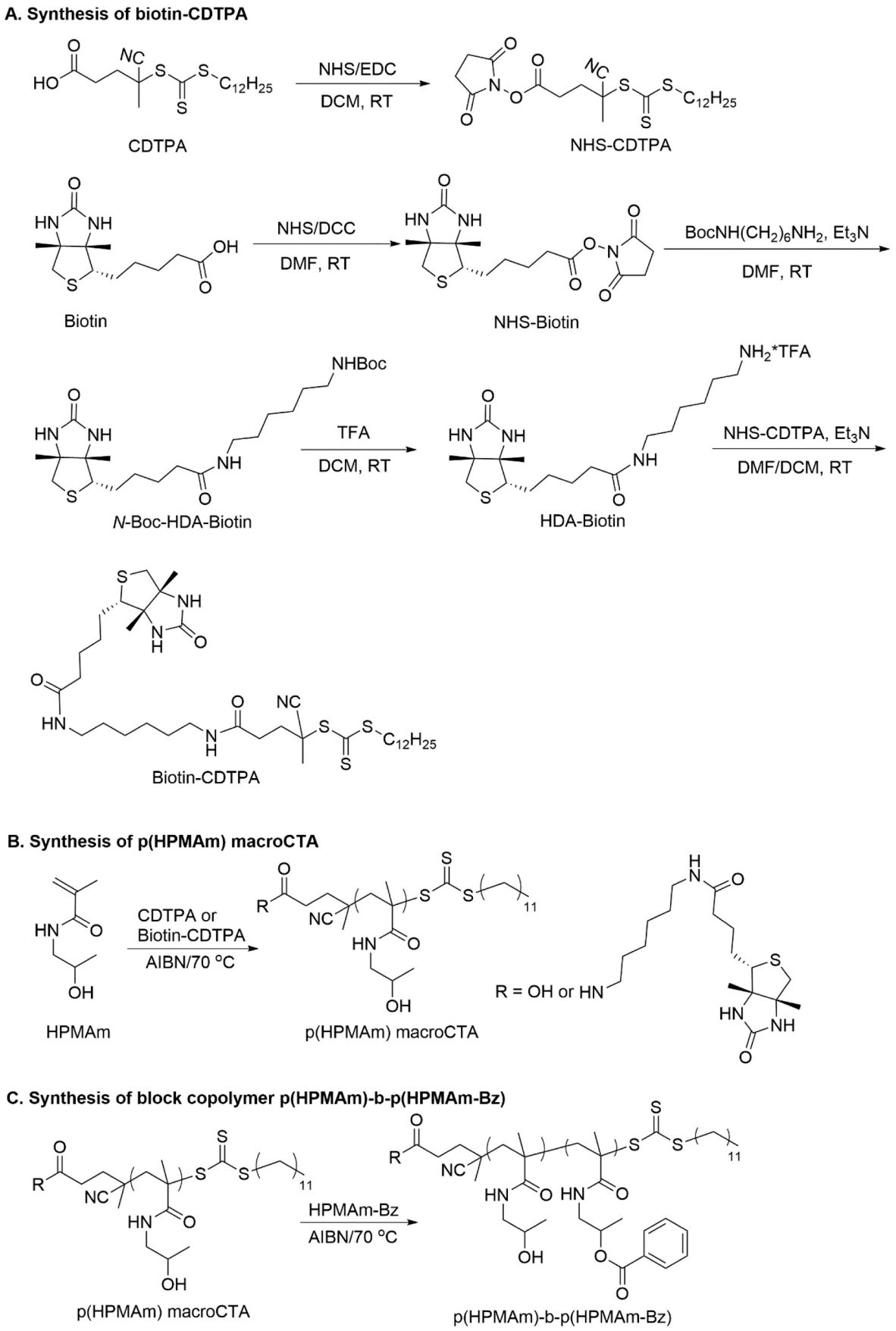

Scheme 1. Synthesis of p(HPMAm)-b-p(HPMAm-Bz) block copolymer with or without a biotin terminus. (**A**) Synthesis of biotin-functionalized chain transfer agent, biotin-CDTPA. (**B**) Synthesis of macro chain trasnfer agent, p(HPMAm). (**C**) Synthesis of block copolymer p(HPMAm)-b-p(HPMAm-Bz).

outcomes were not observed when either vitamin B_{12} or folate were used as targeting agents [23,24]. Therefore, biotin has emerged as a remarkable active targeting ligand for nanocarriers [25–29]. Biotin has a valeric acid tail, through which it can be conjugated to other molecules to achieve biotinylation (Scheme 1A) [30]. Biotin can be decorated on the surface of nanocarriers either through pre-conjugation of biotin to the polymers before their assembly into nanocarriers [31–33], or by attaching biotin onto the surface of nanocarriers after formation (post-conjugation) [34,35].

Poly(ethylene glycol) (PEG) remains the 'gold standard' as hydrophilic shell-forming block in polymeric micelles, due to its high water-solubility and stealth properties that avoids adsorption of opsonins onto the surface of nanocarriers, which in turn reduces unspecific uptake of these particles by mononuclear phagocyte system (MPS) [36,37]. Several formulations based on PEGylated micelles for anti-cancer therapy are currently under evaluation in clinical trials [8,38,39]. However, in contrary to the general assumption that PEGylated substances lack of immunogenicity, it has been shown that repeated injections of PEGylated nanoparticles can induce a phenomenon termed the accelerated blood clearance (ABC) effect, which is mediated by anti-PEG immunoglobulin M antibodies (IgM) [40,41]. Therefore, the search for alternative polymers that do not result in an immune response but maintain the long circulation is required. p(HPMAm) is a promising alternative for PEG, besides good hydrophilicity and biocompatibility, because of its multifunctionality, which enables modification with either hydrophobic moieties to serve as a micellar core, or conjugated with multiple drugs and bioactive ligands for targeted delivery [42–47]. Importantly, Szoka et al. reported that the ABC phenomenon was not observed upon repeated administration of p(HPMAm) modified liposomes due to the lack of formation of anti-p(HPMAm) IgM antibodies in rats, whereas a pronounced IgM response was observed for animals repeatedly treated with PEG-coated liposomes [48].

Recently the synthesis of poly(ethylene glycol)-*block*-poly(*N*-2-benzoyloxypropyl methacrylamide) (mPEG-b-p(HPMAm-Bz)) was reported [49]. These micelles showed high stability, drug loading and drug retention as a result of π-π stacking interactions between the aromatic groups of the drugs and the polymer chains. In the same study it was shown that paclitaxel (PTX)-loaded mPEG-b-p(HPMAm-Bz) micelles exhibited high therapeutic efficacy and complete tumor regression in mice bearing human epidermoid and breast carcinoma xenografts. Taken this in mind, we here set out to develop a biotin-decorated fully p(HPMAm)-based anti-cancer drug delivery system. To this end, p(HPMAm)-b-p(HPMAm-Bz) block copolymers with and without biotin modification were synthesized by reversible addition−fragmentation chain-transfer (RAFT) polymerization and used for the formation of biotinylated micelles. The cellular uptake and cytotoxicity of these micelles loaded with PTX were evaluated using A549 human lung cancer cells overexpressing the biotin receptor as well as in HEK293 kidney cells lacking this receptor.

2. Materials and methods

2.1. Materials

D-(+)-Biotin was purchased from Santa Cruz Biotechnology, Inc. (Heidelberg, Germany). *N*-Hydroxysuccinimide (NHS), dicyclohexylcarbodiimide (DCC), *N*-Boc-1,6-hexanediamine, triethylamine (TEA), trifluoroacetic acid (TFA), 4-cyano-4-[(dodecylsulfanylthiocarbonyl)-sulfanyl]pentanoic acid (CDTPA), *N*-(3-dimethylaminopropyl)-*N*′-ethylcarbodiimide hydrochloride (EDC), sodium bicarbonate ($NaHCO_3$), sodium chloride (NaCl), anhydrous sodium sulfate (Na_2SO_4), 4-(2-hydroxyethyl)piperazine-1-ethanesulfonic acid (HEPES), pyrene, and Dulbecco's modified Eagle's medium (DMEM) were obtained from Sigma-Aldrich (Zwijndrecht, the Netherlands) and used without further purification. Dimethylformamide (DMF, peptide synthesis grade), dichloromethane (DCM, peptide synthesis grade), tetrahydrofuran (THF, HPLC grade), dimethylacetamide (DMAc, peptide synthesis grade), 2-propanol, diethyl ether, and acetone were purchased from Biosolve Ltd. (Valkenswaard, the Netherlands) and used as received, unless indicated otherwise. 2,2′-Azobis(2-methylpropionitrile) (AIBN) was obtained from Sigma-Aldrich (Zwijndrecht, the Netherlands), recrystallized from ethanol and stored at −20 °C. Phosphate buffered saline (PBS, pH 7.4, containing 11.9 mM phosphate, 137 mM sodium chloride, and 2.7 mM potassium chloride) was purchased from Fisher Scientific (Geel, Belgium). Paclitaxel (PTX) was ordered from LC Laboratories (MA, USA). *N*-2-Hydroxypropyl methacrylamide (HPMAm) was synthesized and characterized as described in a previous publication [50]. *N*-2-Benzoyloxypropyl methacrylamide (HPMAm-Bz) was synthesized and characterized as previously reported [43]. PEG standards for gel permeation chromatography (GPC) analysis were supplied by Agilent (Santa Clara, USA). Cyanine 3 (Cy3) amine was supplied by Lumiprobe GmbH (Hannover, Germany). Spectra/Por dialysis membrane (MW 6–8 kDa), DNA stain Hoechst 33430, and reduced serum medium Opti-MEM were obtained from Thermo Fisher Scientific (Landsmeer, the Netherlands), while 0.45 μm RC membrane filters were ordered from Phenomenex (Utrecht, the Netherlands). 3-(4,5-Dimethylthiazol-2-yl)-5-(3-carboxy-methoxyphenyl)-2-(4-sulfophenyl)-2H-tetrazolium (MTS) reagent was purchased from Benelux B.V. (Leiden, the Netherlands).

2.2. Synthesis of the biotin-functionalized RAFT chain transfer agent (biotin-CDTPA)

2.2.1. Synthesis of (+)-biotinyl-N-hydroxysuccinimide (NHS-biotin)

Biotin was activated according to literature procedures [51,52]. In brief, biotin (5.00 g, 20.5 mmol) and NHS (2.83 g, 24.6 mmol) were dissolved in dry DMF (150 mL) at 60 °C. DCC (5.07 g, 24.6 mmol) was added after cooling down to room temperature. The solution was stirred overnight at room temperature. Next, the formed reaction product dicyclohexylurea (DCU) was filtered off and washed with DMF. The combined filtrates were dropped into cold diethyl ether to precipitate the crude product which was then refluxed in 2-propanol, filtered, and dried under vacuum to yield NHS-biotin (4.60 g, 66%). ^{1}H NMR (600 MHz, DMSO-d_6) δ (ppm): 6.43 (s, 1H, N*H*C(=O)), 6.37 (s, 1H, N*H*C(=O)), 4.31 (ddt, 1H, J = 7.5, 5.1, 1.1 Hz, C*H*NHC(=O)), 4.15 (ddd, 1H, J = 7.7, 4.4, 1.8 Hz, C*H*NHC(=O)), 3.11 (ddd, 1H, J = 8.3, 6.3, 4.4 Hz, C*H*S), 2.83—2.86 (m, 1H, CH_2S), 2.78—2.83(m, 4H, (O=)C(CH_2)$_2$C(=O)), 2.65—2.70 (m, 2H, CH_2C(=O)), 2.59 (d, 1H, J = 12.4 Hz, CH_2S), 1.38—1.69 (m, 6H, (CH_2)$_3$CH$_2$C(=O)). ESI-MS m/z 363.0 $(M + Na)^+$, calculated for $C_{14}H_{19}N_3O_5S$ 341.4.

2.2.2. Synthesis of tert-butyl(6-(5-((3aS,4S,6aR)-2-oxohexahydro-1H-thieno[3,4-d]imidazol-4-yl)pentanamido)hexyl)carbamate (N-Boc-HDA-biotin)

N-Boc-HDA-biotin was synthesized as described in previous publications [53,54]. Briefly, NHS-biotin (3.00 g, 8.8 mmol) and *N*-Boc-1,6-hexanediamine (1.90 g, 8.8 mmol) were dissolved in anhydrous DMF (150 mL) and then TEA (1.22 mL, 12.0 mmol) was added. The reaction mixture was stirred at room temperature overnight. The product was isolated by precipitation in cold diethyl ether, dried under vacuum to yield *N*-Boc-HDA-biotin (3.50 g, 90%). ^{1}H NMR (600 MHz, DMSO-d_6) δ (ppm): 7.72 (t, 1H, J = 5.6 Hz, N*H*), 6.75 (t, 1H, J = 5.8 Hz, N*H*), 6.41 (s, 1H, NH-biotin), 6.35 (s, 1H, NH-biotin), 4.30 (ddt, 1H, J = 7.6, 5.2, 1.1 Hz, C*H*NH), 4.12 (ddd, 1H, J = 7.7, 4.4, 1.9 Hz, C*H*NH), 3.09 (ddd, 1H, J = 8.7, 6.2, 4.4 Hz, SC*H*CH$_2$), 3.00 (q, 2H, NCH_2), 2.85—2.90 (m, 2H, NCH_2), 2.82 (dd, 1H, J = 12.4, 5.1 Hz, SCH*H*), 2.57 (d, 1H, J = 12.4 Hz, SC*H*H), 2.04 (t, 2H, J = 7.4 Hz, CH_2C(=O)), 1.38—1.61 (m, 23H, 7CH$_2$, C(CH$_3$)$_3$). ESI-MS m/z 443.2 $(M + H)^+$, 465.2 $(M + Na)^+$, calculated for $C_{21}H_{38}N_4O_4S$ 442.6.

2.2.3. Synthesis of N-(6-aminohexyl)-5-((3aS,4S,6aR)-2-oxohexahydro-1H-thieno[3,4-d]imidazole-4-yl)pentanamide trifluoroacetate (HDA-biotin)

The removal of the Boc protection group from *N*-Boc-HDA-biotin was performed following literature procedures [53,54]. In short, to a solution of *N*-Boc-HDA-biotin (3.50 g, 7.9 mmol) in DCM (43 mL), TFA (8.5 mL, 111.0 mmol) was added. The mixture was stirred at room temperature for 3 h. The solvent was evaporated under reduced pressure to yield a yellowish oil. The crude product was subsequently precipitated in an excess of cold diethyl ether. After repeatedly dissolving in methanol and evaporation under vacuum to remove residual TFA, the oil was dissolved in 10 mL water and lyophilized to yield HDA-biotin (3.50 g, 97%). ^{1}H NMR (600 MHz, DMSO-d_6) δ (ppm): 7.75 (t, J = 5.6 Hz, 1H, NH), 7.40 (br, 3H, NH_3), 6.43 (s, 1H, NH-biotin), 6.38 (s, 1H, NH-biotin), 4.31 (dd, 1H, J = 7.7, 5.1 Hz, CHNH), 4.12 (ddd, 1H, J = 7.2, 4.4, 1.8 Hz, CHNH), 3.09 (ddd, 1H, J = 8.6, 6.0, 4.4 Hz, $SCHCH_2$), 3.01 (q, 2H, J = 6.6 Hz, NCH_2), 2.81 (dd, 1H, J = 12.4, 5.1 Hz, SCHH), 2.74—2.78 (m, 2H, NH_2CH_2), 2.57 (d, 1H, J = 12.5 Hz, SCHH), 2.04 (t, 2H, J = 7.4 Hz, $CH_2C(=O)$), 1.22—1.61 (m, 14H, $7CH_2$). ESI-MS m/z 343.2 $(M + H)^+$, calculated for $C_{16}H_{30}N_4O_2S$ 342.5.

2.2.4. Synthesis of 4-cyano-4-[(dodecylsulfanylthiocarbonyl)-sulfanyl] pentanoic succinimide (NHS-CDTPA)

The synthesis of NHS-CDTPA was based on previously published papers [55,56]. Shortly, to a solution of 4-cyano-4-[(dodecylsulfanylthiocarbonyl)-sulfanyl]pentanoic acid (CDTPA) (5.00 g, 12.4 mmol) in 50 mL dry DCM at 0 °C, NHS (1.80 g, 15.6 mmol) and EDC (3.02 g, 15.9 mmol) were added. The reaction mixture was stirred at 0 °C for 1 h and then at room temperature for 9 h. Subsequently, the DCM solution was washed with saturated $NaHCO_3$ (aq.) and the resulting DCM phase was dried over anhydrous Na_2SO_4. After 2 h, Na_2SO_4 was filtered off and the solvent was removed under reduced pressure and further dried under vacuum to yield NHS-CDTPA (5.30 g, 85%). ^{1}H NMR (600 MHz, chloroform-*d*) δ (ppm): 3.33 (m, 2H, CH_2CH_2S), 2.93 (ddd, J = 9.2, 6.3, 3.9 Hz, 2H, $CH_2C(=O)$), 2.85 (s, 4H, $(O=)C(CH_2)_2C(=O)$), 2.66 (ddd, 1H, J = 14.4, 9.8, 6.5 Hz, $CH_2CH_2C(=O)$), 2.53 (ddd, 1H, J = 14.4, 9.8, 6.5 Hz, $CH_2CH_2C(=O)$), 1.88 (s, 3H, $C(CH_3)$), 1.70 (tt, 2H, J = 12.8, 3.9 Hz, CH_2CH_2S), 1.37—1.42 (m, 2H, $CH_2(CH_2)_2S$), 1.23—1.31 (m, 16H, $CH_3(CH_2)_8CH_2$), 0.88 (t, J = 7.0 Hz, 3H, $CH_3CH_2CH_2$). ESI-MS m/z 559.2 $(M + Na + 2H_2O)^+$, 541.2 $(M + Na + H_2O)^+$, calculated for $C_{23}H_{36}N_2O_4S_3$ 500.7.

2.2.5. Synthesis of biotin-functionalized chain transfer agent (biotin-CDTPA)

Coupling of NHS-CDTPA with HDA-biotin afforded a RAFT chain transfer agent, biotin-CDTPA. Briefly, to a solution of HDA-biotin (658 mg, 1.4 mmol) in a mixture of 18 mL anhydrous DMF and DCM (1:1, *v*/v), NHS-CDTPA (656 mg, 1.3 mmol) and TEA (450 μL, 3.3 mmol) were added. The reaction mixture was stirred at room temperature for 16 h. Next, DCM was evaporated under vacuum at 40 °C, and subsequently the reaction mixture was dropped into a large excess of reverse osmosis (RO) water to precipitate the crude product which was then washed with 2-propanol, filtered and dried under vacuum to yield biotin-CDTPA (~900 mg, 94%). ^{1}H NMR (600 MHz, DMSO-d_6) δ (ppm): 7.96 (t, 1H, J = 5.6 Hz, NH), 7.73 (t, 1H, J = 5.6 Hz, NH), 6.41 (s, 1H, NH-biotin), 6.35 (s, 1H, NH-biotin), 4.30 (dd, 1H, J = 7.8, 5.1 Hz, CHNH), 4.12 (ddd, 1H, J = 7.6, 4.5, 1.8 Hz, CHNH), 3.09 (ddd, 1H, J = 8.7, 6.0, 4.4 Hz, $SCHCH_2$), 3.04—2.98 (m, 4H, $2NHCH_2$), 2.82 (dd, 1H, J = 12.4, 5.1 Hz, SCHH), 2.58 (d, 1H, J = 12.4 Hz, SCHH), 2.43—2.26 (m, 4H, $2CH_2C(=O)$), 2.04 (t, 2H, J = 7.4 Hz, CH_2CH_2S), 1.85 (s, 3H, $C(CH_3)$), 1.63—1.20 (m, 36H, $18CH_2$), 0.85 (t, 3H, J = 6.9 Hz, $CH_3CH_2CH_2$). ESI-MS m/z 728.3 $(M + H)^+$, 750.2 $(M + Na)^+$, calculated for $C_{35}H_{61}N_5O_3S_4$ 728.2.

2.3. Synthesis and characterization of p(HPMAm)-b-p(HPMAm-Bz) block copolymers with or without biotin terminus

2.3.1. Synthesis of poly[N-(2-hydroxypropyl) methacrylamide] macro chain transfer agent (p(HPMAm) macroCTA) with or without biotin terminus

The p(HPMAm) macroCTA with or without a biotin terminus was synthesized using RAFT polymerization with CDTPA or biotin-CDTPA as CTA and AIBN as initiator at 70 °C [57]. In detail, the reagents were weighed in Schlenk tubes and subsequently dissolved in dry DMAc (10 mL). The concentration of HPMAm was 300 mg/mL. To obtain p(HPMAm) of different molecular weights, molar ratios of [HPMAm]/[CDTPA]/[AIBN] of 180/5/1, 320/5/1 and 460/5/1 were applied. For the polymerization of HPMAm with a biotin terminal end, the molar ratio of [HPMAm]/[biotin-CDTPA]/[AIBN] was 460/5/1. The obtained solutions were degassed by three cycles of freeze-vacuum-thaw, backfilled with nitrogen, and the tubes were subsequently immersed in a prewarmed oil bath at 70 °C. At different time points, samples were withdrawn and analyzed by ^{1}H NMR and GPC. The reaction was carried out for 5–6 h. Next, the polymers were isolated by precipitation in diethyl ether for three times (DMAc/diethyl ether = 1/49, *v*/v) and dried overnight under vacuum to give the final products (entries 1–4 in Table 1).

2.3.2. Synthesis of block copolymers of poly[N-(2-hydroxypropyl) methacrylamide]-block-[N-(2-benzoyloxy-propyl) methacrylamide] (p(HPMAm)-b-p(HPMAm-Bz)) with or without biotin terminus

The obtained p(HPMAm) macroCTAs with or without biotin terminus were chain-extended with HPMAm-Bz under the same conditions as for the synthesis of p(HPMAm). In detail, the reagents were weighed in Schlenk tubes and subsequently dissolved in dry DMAc (7 mL). The concentration of HPMAm-Bz was 300 mg/mL. For the synthesis of copolymers with different molecular weights of the hydrophilic and hydrophobic blocks, the molar ratios of [HPMAm-Bz]/[p(HPMAm)]/[AIBN] were 250/5/1, 500/5/1 and 900/5/1, respectively. For the synthesis of biotinylated copolymer, the molar ratio of [HPMAm-Bz]/[biotinylated p(HPMAm)]/[AIBN] was 900/5/1. The solution was degassed by three cycles of freeze-vacuum-thawing, backfilled with nitrogen, and then the tube was immersed in a prewarmed oil bath at 70 °C. At different time points, samples were withdrawn and analyzed by ^{1}H NMR and GPC. The reaction was carried out for 18–20 h. The polymers were isolated by precipitation in diethyl ether for three times (DMAc/diethyl ether = 1/49, *v*/v) and dried overnight under vacuum to give the final products (entries 5–14 in Table 1).

2.3.3. Characterizations of the polymers by ^{1}H NMR spectroscopy and GPC

^{1}H NMR spectra were recorded using a Bruker 600 MHz spectrometer (Billerica, MA, USA). The polymers (5–10 mg) were dissolved in 600 μL DMSO-d_6. The DMSO-d_6 peak at 2.50 ppm was used as the reference line.

Chemical shifts of p(HPMAm) (Fig. S2B): 7.18 (b, $C(=O)NHCH_2$), 4.70 (s, $CH(CH_3)OH$), 3.68 (s, $NHCH_2CH(CH_3)$ OH), 2.9 (b, $NHCH_2CH$), 0.4—2.0 (b, the rest of protons are from the methyl and backbone CH_2 protons). Chemical shifts of the biotinylated p(HPMAm) (Fig. S3B): in addition to protons from p(HPMAm), 7.89 (s, NH-linker), 7.74 (s, NH-linker), 6.43 (NH-biotin), 6.37 (NH-biotin), 4.30 (CHNH), 4.14 (CHNH).

The theoretical number average of molecular weight ($M_{n,\ theory}$) of p(HPMAm) with or without biotin terminus was calculated using the following Eq. (1):

$$M_{n,theory} = [monomer]/[CTA] \times conversion \times M_{monomer} + M_{CTA} \quad (1)$$

where the conversion of HPMAm was determined by comparing the integration areas of resonances from the vinyl protons of HPMAm at 5.30 ppm and the methine protons of HPMAm at 3.68 ppm (Fig. S2A & 3A), and [monomer], [CTA], $M_{monomer}$ and M_{CTA} are the initial

Table 1
Characteristics of the polymers synthesized by RAFT as determined by ^{1}H NMR, GPC and fluorometric analysis.

En-try	Polymers	Molar Ratio of M/CTA/I	Monomer Conversion (%)	$M_{n,\ theory}$ (kDa)[a]	$M_{n,\ NMR}$ (kDa)[b]	$M_{n,\ GPC}$ (kDa)[c]	PDI[c]	CMC (μg/mL)[d]
1	$p(HPMAm)_{3.0k}$	180:5:1	51	3.0	–	3.2	1.19	–
2	$p(HPMAm)_{4.9k}$	320:5:1	50	4.9	–	5.0	1.22	–
3	$p(HPMAm)_{7.1k}$	460:5:1	51	7.1	–	7.7	1.26	–
4	biotinylated $p(HPMAm)_{6.8k}$	460:5:1	46	6.8	7.0	8.1	1.33	–
5	$p(HPMAm)_{3.0k}$-b-$p(HPMAm\text{-}Bz)_{5.4k}$	250:5:1	36	7.5	8.4	6.6	1.39	33
6	$p(HPMAm)_{3.0k}$-b-$p(HPMAm\text{-}Bz)_{9.9k}$	500:5:1	39	12.6	12.9	8.7	1.43	27
7	$p(HPMAm)_{3.0k}$-b-$p(HPMAm\text{-}Bz)_{15.6k}$	900:5:1	44	22.5	18.6	10.6	1.55	21
8	$p(HPMAm)_{4.9k}$-b-$p(HPMAm\text{-}Bz)_{6.4k}$	250:5:1	42	10.1	11.3	7.4	1.36	32
9	$p(HPMAm)_{4.9k}$-b-$p(HPMAm\text{-}Bz)_{11.3k}$	500:5:1	38	14.3	16.2	9.2	1.41	22
10	$p(HPMAm)_{4.9k}$-b-$p(HPMAm\text{-}Bz)_{16.8k}$	900:5:1	40	22.8	21.7	10.0	1.41	6
11	$p(HPMAm)_{7.1k}$-b-$p(HPMAm\text{-}Bz)_{4.9k}$	250:5:1	45	12.7	12.0	9.1	1.42	43
12	$p(HPMAm)_{7.1k}$-b-$p(HPMAm\text{-}Bz)_{9.1k}$	500:5:1	39	16.7	16.2	8.5	1.49	22
13	$p(HPMAm)_{7.1k}$-b-$p(HPMAm\text{-}Bz)_{15.0k}$	900:5:1	39	24.9	22.1	11.0	1.48	6
14	biotinylated $p(HPMAm)_{6.8k}$-b-$p(HPMAm\text{-}Bz)_{16.3k}$	900:5:1	41	25.3	23.1	12.9	1.48	–
15	Cy3-labeled $p(HPMAm)_{4.9k}$-b-$p(HPMAm\text{-}Bz)_{18.7k}$[e]	–	–	–	23.6	10.0	1.41	–

[a] $M_{n,\ theory}$ calculated using Eqs. (1) and (3);
[b] $M_{n,\ NMR}$ calculated using Eqs. (2) and (4);
[c] Determined by GPC analysis (DMF containing 10 mM LiCl as eluent, PEGs as standards), PDI, equal to $M_{w,\ GPC}/M_{n,\ GPC}$;
[d] Determined using pyrene fluorescence method;
[e] Obtained by labeling of $p(HPMAm)_{4.9k}$-b-$p(HPMAm\text{-}Bz)_{16.8k}$ (Section 2.4).

monomer and CTA concentrations, molecular weights of monomer (M_{HPMAm} = 143 g/mol) and CTA (M_{CDTPA} = 403 g/mol, $M_{biotin\text{-}CDTPA}$ = 727 g/mol), respectively.

The number average of molecular weight determined by ^{1}H NMR analysis ($M_{n,\ NMR}$) of biotinylated p(HPMAm) was calculated using the following Eq. (2):

$$M_{n,NMR} = \text{degree of polymerization} \times M_{monomer} + M_{CTA} \quad (2)$$

where the degree of polymerization of biotinylated p(HPMAm) was determined by comparing the integration areas of resonances from the methine protons of biotin-CDTPA at 4.14 ppm and the methine protons of biotinylated p(HPMAm) at 3.68 ppm (Fig. S3B), and $M_{monomer}$ and M_{CTA} are molecular weights of monomer (M_{HPMAm} = 143 g/mol) and CTA ($M_{biotin\text{-}CDTPA}$ = 727 g/mol), respectively.

Chemical shifts of p(HPMAm)-b-p(HPMAm-Bz) with or without biotin terminus (Fig. S4B & 5B): in addition to protons from p(HPMAm) with or without biotin terminus, 7.93 (s, aromatic CH), 7.34—7.65 (b, aromatic CH), 5.00 (s, $NHCH_2C\underline{H}(CH_3)O(O=C)$), 3.15 (b, $NHC\underline{H_2}CH(CH_3)O(O=C)$).

$M_{n,\ theory}$ of p(HPMAm)-b-p(HPMAm-Bz) with or without biotin terminus was calculated using the following Eq. (3):

$$M_{n,theory} = [monomer]/[macroCTA] \times conversion \times M_{monomer} + M_{n,macroCTA} \quad (3)$$

where the conversion of HPMAm-Bz was determined by comparing the integration areas of resonances from the methine protons of p(HPMAm-Bz) at 5.00 ppm and the vinyl protons of HPMAm-Bz at 5.60 ppm (Fig. S4A & 5A), and [monomer], [macroCTA], $M_{monomer}$ and $M_{n,\ macroCTA}$ are the initial monomer and macroCTA concentrations, molecular weights of monomer ($M_{HPMAm\text{-}Bz}$ = 247 g/mol) and macroCTA ($M_{n,\ p(HPMAm)}$ = 3000, 4900, and 7100 g/mol, $M_{n,\ biotinylated\ p(HPMAm)}$ = 6800 g/mol), respectively.

$M_{n,\ NMR}$ of p(HPMAm)-b-p(HPMAm-Bz) with or without biotin terminus was calculated using the following Eq. (4):

$$M_{n,NMR} = \text{degree of polymerization} \times M_{monomer} + M_{n,macroCTA} \quad (4)$$

where the degree of polymerization of p(HPMAm)-b-(pHPMAm-Bz) with or without biotin terminus was determined by comparing the integration areas of resonances from the methine protons of p(HPMAm-Bz) at 5.00 ppm and the methine protons of p(HPMAm) with or without biotin terminus at 3.68 ppm (Fig. S4B & 5B), and $M_{monomer}$ and $M_{n,\ macroCTA}$ are molecular weights of monomer ($M_{HPMAm\text{-}Bz}$ = 247 g/mol) and macroCTA ($M_{n,\ p(HPMAm)}$ = 3000, 4900, and 7100 g/mol, $M_{n,\ biotinylated\ p(HPMAm)}$ = 6800 g/mol), respectively.

GPC was carried out to determine the number average molecular weight (M_n), weight average molecular weight (M_w) and dispersity of molecular weight (PDI, equal to M_w/M_n) using two serial PLgel 5 μm MIXED-D columns and PEGs of narrow molecular weight distribution as calibration standards [58]. Samples were prepared by dissolving approximately 10 mg of the polymer in 3 mL of DMF and samples of 50 μL were injected onto the column. The eluent was DMF containing 10 mM LiCl, the elution rate was 1 mL/min, the temperature was 65 °C, and detection was done using a refractive index (RI) detector and ultraviolet (UV) detector at the wavelength of 254 and 309 nm.

2.4. Synthesis and characterizations of cyanine3 (Cy3)-labeled p(HPMAm)-b-p(HPMAm-Bz) block copolymer

The terminal carboxylic acid group of the p(HPMAm) block of p(HPMAm)-b-p(HPMAm-Bz) was first activated by NHS/EDC, yielding p(HPMAm)-b-p(HPMAm-Bz) NHS ester, followed by its reaction with the primary amine groups of Cy3 [59]. In detail, p(HPMAm)-b-p(HPMAm-Bz) (100 mg, thus 0.0046 mmol COOH end groups, entry 10 in Table 1) was dissolved in 1 mL dry DMAc and subsequently EDC (1.3 mg, 0.0069 mmol) and NHS (0.8 mg, 0.0069 mmol) dissolved in 1 mL DCM were added. The reaction mixture was stirred at room temperature for 1 h followed by addition of Cy3 amine (3.5 mg, 0.0056 mmol) dissolved in 0.5 mL dry DCM also containing TEA (8.0 μL, 0.058 mmol), and the resulting reaction mixture was stirred at room temperature overnight and subsequently transferred into a Spectra/Por dialysis membrane with a molecular weight cutoff of 6–8 kDa and sealed. Dialysis was carried out for 48 h against water/THF (1:1 *v*/v) which was changed every 12 h [49]. The final product (entry 15 in Table 1) was collected after lyophilization and characterized by ^{1}H NMR and GPC coupled with a UV detector (detection wavelength of 550 nm) as described in Section 2.3.3. The labeling efficiency was determined by Jasco FP8300 Spectrofluorometer (Easton, MD, USA) with a calibration curve of Cy3 amine in DMF at the concentration of 0.0625, 0.125, 0.25, 0.5 and 1 μg/mL. Fluorescence emission spectra of Cy3 from 500 to 800 nm were recorded at room temperature with an excitation wavelength at

550 nm. The excitation and emission band slits were 2.5 nm.

2.5. Preparation and characterizations of empty (Cy3-labeled) and PTX-loaded p(HPMAm)-b-p(HPMAm-Bz) micelles with or without biotin modification

2.5.1. Preparation of empty (Cy3-labeled) and PTX-loaded p(HPMAm)-b-p(HPMAm-Bz) micelles

Empty p(HPMAm)-b-p(HPMAm-Bz) micelles (with or without biotin modification) were prepared by solvent extraction method. In detail, 1 mL DMF solution of 18.0 mg of nonbiotinylated p(HPMAm)-b-p(HPMAm-Bz) copolymer (entry 13 in Table 1) and 2.0 mg of biotinylated p(HPMAm)-b-p(HPMAm-Bz) copolymer (entry 14 in Table 1), or 20.0 mg nonbiotinylated p(HPMAm)-b-p(HPMAm-Bz) copolymer only (entry 13 in Table 1) was pipetted into 1 mL Milli-Q water while stirring for 1 min. To remove DMF, the solution was transferred into a Spectra/Por dialysis membrane with a molecular weight cutoff of 6–8 kDa and sealed. Dialysis was carried out for 24 h against Milli-Q water which was changed at 2nd, 5th and 13th h. Next, the micellar dispersion was filtered through 0.45 μm RC membrane filter. The size of the empty p(HPMAm)-b-p(HPMAm-Bz) micelles was determined by dynamic light scattering (DLS) after 10-fold dilution in water at 25 °C using a Zetasizer Nano S at a fixed angle of 173° (Malvern Instruments Ltd., Malvern, UK). The *Z*-average diameter (Z_{ave}) and polydispersity index (PDI) were calculated by the Zetasizer software v.7.13. The zeta-potential of the empty p(HPMAm)-b-p(HPMAm-Bz) micelles was measured after 10-fold dilution in 10 mM HEPES buffer pH 7.4 using a Zetasizer Nano Z (Malvern Instruments Ltd., Malvern, UK). The residual DMF content of the micellar dispersion was measured by ^{1}H NMR as follows. Two hundred μL micelle dispersion was mixed with 400 μL D_2O, and no any peak corresponding to DMF was detected (detection limit ~50 ppm).

PTX-loaded micelles were prepared similarly as for empty micelles. In detail, 1 mL DMF in which the polymers (20 mg/mL, entries 13 and/or 14 in Table 1) and PTX (concentrations ranging from 1 to 25 mg/mL) were dissolved was rapidly pipetted into 1 mL Milli-Q water while stirring for 1 min, and DMF was subsequently removed by dialysis followed by filtration through 0.45 μm RC membrane filter to remove non-encapsulated PTX. To determine the drug content of PTX-loaded micelles, the micellar dispersions were diluted 10-fold with THF (HPLC grade) to destabilize the micelles, and the dissolved PTX was subsequently quantified by HPLC analysis (Waters Alliance System). The elution was isocratic with a mobile phase of THF/water = 55:45 (*v*/v) containing 0.1% formic acid. The total run time was 8 min with a flow rate of 1 mL/min. A Sunfire C18 column (5 μm, 4.6 × 150 mm) was used and the detection wavelength was 227 nm. The injection volume was 10 μL and the PTX concentration in the different samples was calculated using a calibration curve of PTX standards prepared in THF in a concentration range of 6–100 μg/mL. The encapsulation efficiency (EE) and loading capacity (LC) were calculated by the following formulas:

$$\text{EE} = \frac{\text{amountofloaded PTX}}{\text{amountof PTX usedforloading}} \times 100\% \quad (5)$$

$$\text{LC} = \frac{\text{amountofloaded PTX}}{\text{amountofloaded PTX} + \text{amountofobtainedpolymer}} \times 100\% \quad (6)$$

To study cellular uptake, empty Cy3-labeled p(HPMAm)-b-p(HPMAm-Bz) micelles (with or without biotin modification) were prepared similarly as for empty micelles without Cy3 label. Briefly, 1 mL DMF solution of 17.4 mg of nonbiotinylated p(HPMAm)-b-p(HPMAm-Bz) copolymer (entry 13 in Table 1), 2.0 mg of biotinylated p(HPMAm)-b-p(HPMAm-Bz) copolymer (entry 14 in Table 1) and 0.6 mg Cy3-labeled p(HPMAm)-b-p(HPMAm-Bz) (entry 15 in Table 1), or 19.4 mg nonbiotinylated p(HPMAm)-b-p(HPMAm-Bz) (entry 13 in Table 1) and 0.6 mg Cy3-labeled p(HPMAm)-b-p(HPMAm-Bz) (entry 15 in Table 1) was rapidly pipetted into 1 mL Milli-Q water while stirring for 1 min, and DMF was subsequently removed by dialysis followed by filtration through 0.45 μm RC membrane filter.

2.5.2. P(HPMAm)-b-p(HPMAm-Bz) polymer concentration determination

The polymer concentrations in the micellar dispersions were determined by GPC analysis (Waters Alliance System) after 10-fold dilution with DMF to destabilize the micelles. The elution was isocratic with a mobile phase of DMF containing 10 mM LiCl. Two serial PLgel 5 μm MIXED-D columns were used. Total run time was 30 min with a flow rate of 1 mL/min, the injection volume was 50 μL, the column temperature was 65 °C, and detection was done using a refractive index (RI) detector and ultraviolet (UV) detector at the wavelength of 254 and 309 nm. The polymer concentrations in the different samples were calculated using a calibration curve of samples of polymer dissolved in DMF at concentrations between 0.1 and 2 mg/mL. The micelle recovery yield was calculated by the following formula (7):

$$\text{Recovery yield} = \frac{\text{amountofobtainedpolymer}}{\text{amountofpolymerusedforprepearation}} \times 100\% \quad (7)$$

2.5.3. In vitro stability of p(HPMAm)-b-p(HPMAm-Bz) micelles

The in vitro colloidal stability of empty micelles, empty p(HPMAm)-b-p(HPMAm-Bz) (entry 13 in Table 1) micelles (with or without biotin decoration), prepared as described in Section 2.5.1 and diluted 10-fold with PBS pH 7.4 (final polymer concentration was 0.9 and 0.6 mg/mL for biotinylated and nonbiotinylated micelles), was investigated. The samples were incubated at 37 °C for 48 h. Small sample aliquots were analyzed by DLS.

2.5.4. Effect of the hydrophobic/hydrophilic block molecular weight ratio of p(HPMAm)-b-p(HPMAm-Bz) on micelle size

The effect of hydrophobic/hydrophilic block molecular weight ratio of p(HPMAm)-b-p(HPMAm-Bz) on the size of the formed micelles was investigated using the small library of copolymers synthesized as described in Section 2.3 (entries 5–13 in Table 1). The different diblock copolymers (20 mg) were dissolved in 1 mL DMF and the obtained solutions were rapidly pipetted into 1 mL Milli-Q water while stirring for 1 min. DMF was removed by dialysis, and the obtained micellar dispersions were subsequently filtered through 0.45 μm RC membrane filter. The size of micelles was determined by DLS.

2.6. Critical micelle concentration (CMC) determination

The CMCs of the different p(HPMAm)-b-p(HPMAm-Bz) block copolymers were determined using pyrene fluorescence method as described previously [60,61]. Briefly, the p(HPMAm)-b-p(HPMAm-Bz) micelles were prepared by the solvent extraction method as described in Section 2.5.1, and the p(HPMAm)-b-p(HPMAm-Bz) polymer concentration was determined as described in Section 2.5.2. Subsequently, the micelle dispersions were diluted with distilled water to obtain concentrations that ranged from 1.0×10^{-5} to 1 mg/mL. Next, 50 μL of pyrene dissolved in acetone (0.18 mM) was added to 500 μL of the polymer dispersion. The dispersions were incubated at room temperature overnight to evaporate acetone. Fluorescence excitation spectra of pyrene from 300 to 360 nm were recorded at 37 °C while the intensity of the emitted light at 390 nm was recorded. The excitation and emission band slits were 10 and 2.5 nm, respectively. The intensity ratio of I_{338}/I_{333} was plotted against the polymer concentration to determine CMC.

2.7. Cell culture

Human adenocarcinoma alveolar based lung cancer cell line (A549) and human embryonic kidney cell line (HEK293) were obtained from the American Type Culture Collection (ATCC, Manassas, Virginia, USA). A549 cells are biotin receptor-positive whereas HEK293 cells are biotin

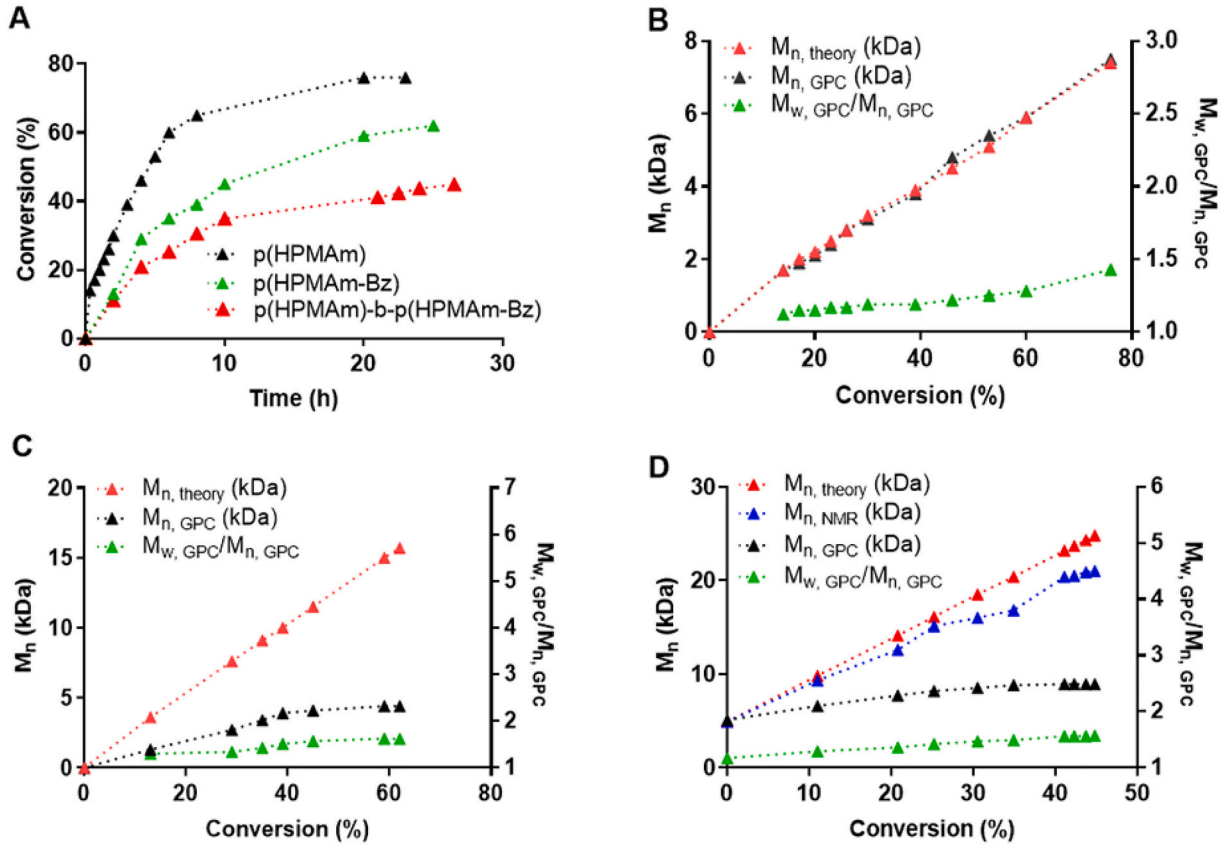

Fig. 1. Conversion as a function of reaction time for the RAFT polymerization of HPMAm and HPMAm-Bz (**A**). M_n (based on GPC and ^{1}H NMR analysis) and $M_{w,\ GPC}/M_{n,\ GPC}$ (PDI) versus conversion of HPMAm and HPMAM-Bz (**B,** p(HPMAm), molar ratio of M/CTA/I was 320/5/1; **C,** p(HPMAm-Bz), molar ratio of M/CTA/I was 500/5/1; and **D,** p(HPMAm)-b-p(HPMAm-Bz), molar ratio of M/macroCTA/I was 900/5/1).

receptor-negative [20]. A549 and HEK293 cells were cultured in DMEM supplemented with 10% of fetal bovine serum (FBS) at 37 °C in a humidified atmosphere containing 5% of CO_2. Both cell lines were grown in 75 cm^2 cell culture flasks and passaged twice a week.

2.8. In vitro cellular uptake of empty Cy3-labeled p(HPMAm)-b-p(HPMAm-Bz) micelles

A549 and HEK293 cells were seeded into 96-well plates at a density of 1×10^4 cells/well and incubated for 24 h at 37 °C in a humidified atmosphere containing 5% of CO_2. Stock solutions of empty Cy3-labeled micelles with or without biotin decoration (polymer concentration was 6 mg/mL) were prepared as described in Section 2.5.1. The cells were incubated with 100 μL of different formulations at 140 μg/mL at 37 °C in a humidified atmosphere containing 5% of CO_2 for 1, 4, 8, and 24 h. Next, Hoechst 33430 was added to the wells 30 min before imaging with a final concentration of 10 nM. The media were replaced with Opti-MEM and the plate was transferred into a Yokogawa CV7000 (Tokyo, Japan) spinning disk microscope with a 40 × 1.2 NA water objective. To investigate whether cellular internalization of the biotinylated micelles indeed occurs via biotin-receptor mediated endocytosis, A549 and HEK293 cells were pre-incubated with 2 mM free biotin for 1 h. Subsequently, the cells were incubated with the Cy3-labeled micelles with or without biotin decoration for 4 h, followed by confocal imaging according to the above procedures.

2.9. In vitro cytotoxicity of empty and PTX-loaded p(HPMAm)-b-p(HPMAm-Bz) micelles

The cell viability was evaluated after 48 h-exposure to the formulations by using the MTS assay. The tetrazolium reagent MTS can be bio-reduced by living cells into a colored formazan product that is soluble in tissue culture medium and that can be quantified by colorimetric method [58,62]. A549 and HEK293 cells were seeded into 96-well plates at a density of 5×10^3 cells/well and incubated for 24 h at 37 °C in a humidified atmosphere containing 5% of CO_2. Stock solutions of empty micelles with biotin decoration (polymer concentration was 9 mg/mL), empty micelles without biotin decoration (polymer concentration was 6 mg/mL), PTX-loaded micelles with biotin decoration (polymer concentration was 7 mg/mL) and PTX-loaded micelles without biotin decoration (polymer concentration was 6 mg/mL) were prepared as described in Section 2.5.1. PTX as Taxol formulation was prepared by dissolving 12 mg of PTX in 1 mL ethanol followed by addition of 1 mL Cremophor EL and sonication for 30 min [43]. A Taxol formulation without PTX was prepared by mixing Cremophor EL and ethanol (1:1, *v*/v). PTX-loaded micellar and Taxol formulations were diluted in cell culture media to yield concentrations of PTX that ranged from 1.0×10^{-5} to 100 μg/mL. The empty micelles were diluted in cell culture medium to yield polymer concentrations ranging from 1.7×10^{-4} to 1700 μg/mL, subsequently, Cremophor EL/ethanol solution was diluted in cell culture medium the same way as the Taxol formulation. The cells were incubated with 100 μL of the different formulations at 37 °C in a humidified atmosphere containing 5% of CO_2 for 48 h. Next, the media were replaced by 100 μL of fresh medium and 20 μL of MTS reagent followed by incubation for 2 h. The cell viability was determined by measuring the absorbance at 492 nm using a Biochrome EZ microplate reader (Jakarta Utara, Indonesia). IC_{50} values were calculated as drug concentration that inhibits the cell growth by 50% after 48 h of cultivation.

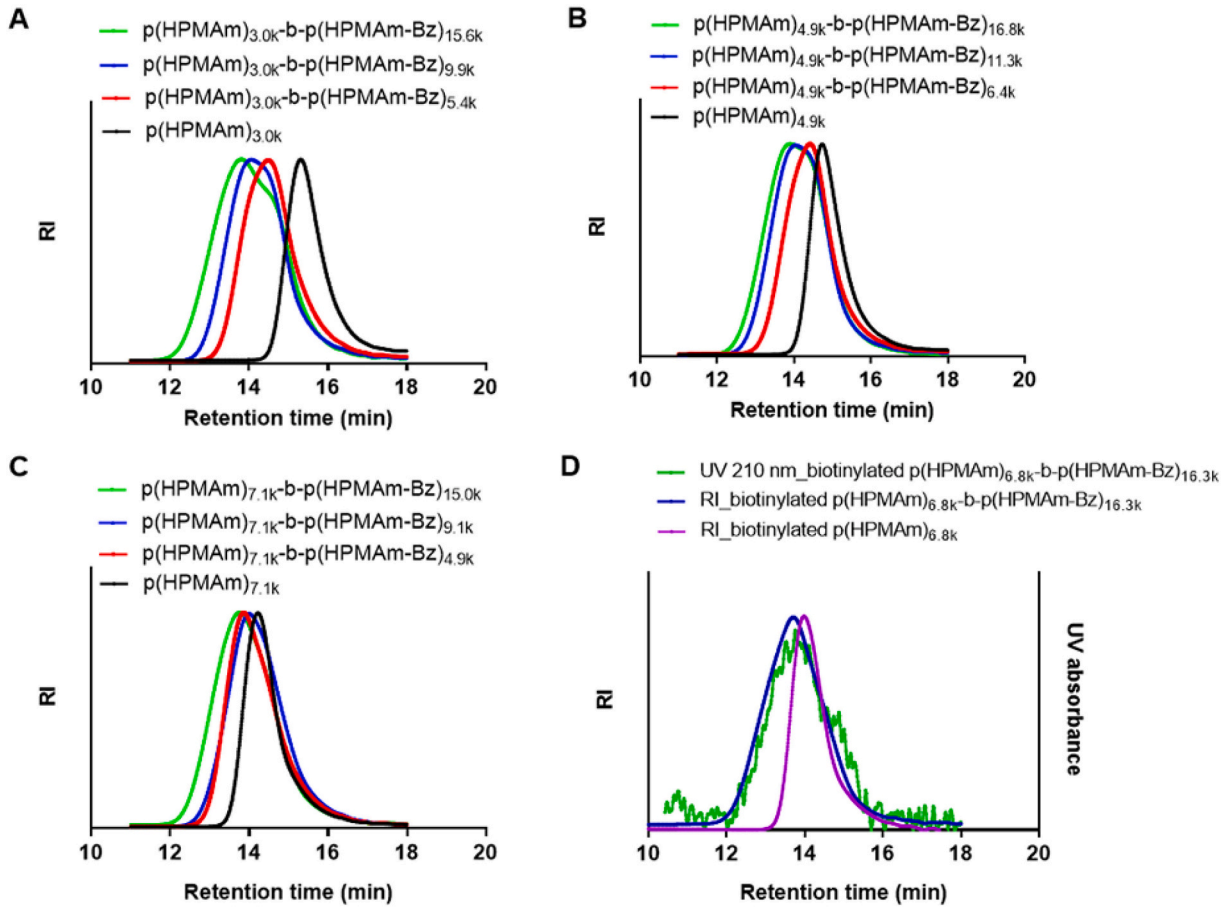

Fig. 2. GPC chromatograms of the synthesized block copolymers. (**A–C**) GPC chromatograms (RI detection) of the different p(HPMAm)-b-p(HPMAm-Bz) copolymers. (**D**) GPC chromatograms (RI and UV detection) of biotinylated p(HPMAm)-b-p(HPMAm-Bz).

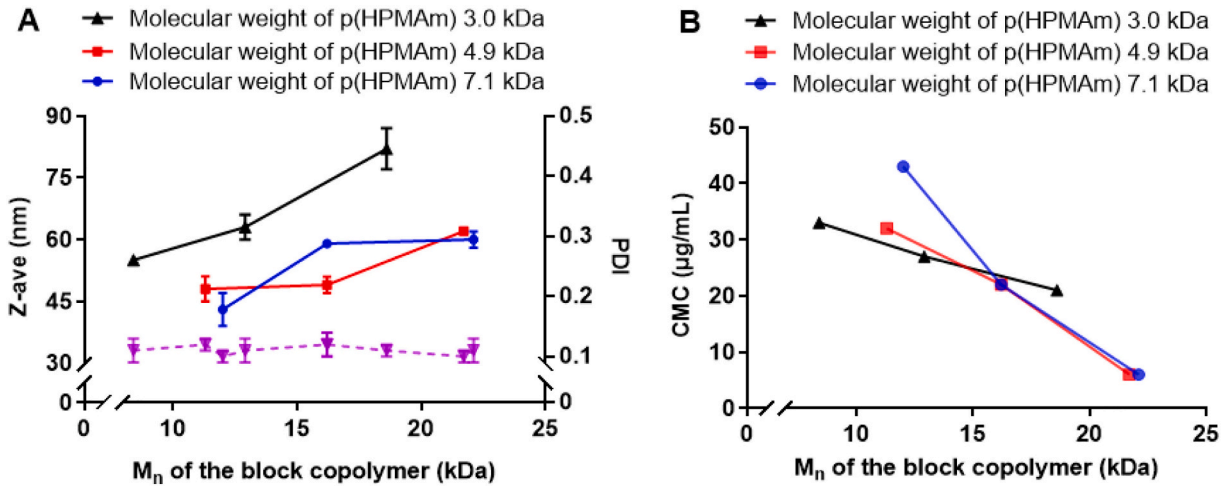

Fig. 3. (**A**) Effect of the molecular weight of the p(HPMAm)-b-p(HPMAm-Bz) block copolymers on the *Z*-average size (black, red, and blue line) and PDI (purple line) of the formed micelles. Data represent mean ± SD ($n = 3$). (**B**) Critical micelle concentration as a function of p(HPMAm)-b-p(HPMAm-Bz) polymer molecular weight. (For interpretation of the references to colour in this figure legend, the reader is referred to the web version of this article.)

2.10. Statistical analysis

Statistical analysis was done by GraphPad Prism 8.3.0 software. Two-way analysis of variance (ANOVA) was used to determine the statistical significance of cell viability data. A value of $p < 0.05$ was considered significant.

3. Results and discussion

3.1. Synthesis of biotin-functionalized chain transfer agent, biotin-CDTPA

A biotin-functionalized RAFT chain transfer agent, namely 4-cyano-4 [(dodecylsulfanylthiocarbonyl)-sulfanyl]pentanoic acid (biotin-CDTPA), was synthesized as shown in Scheme 1A. Amine-

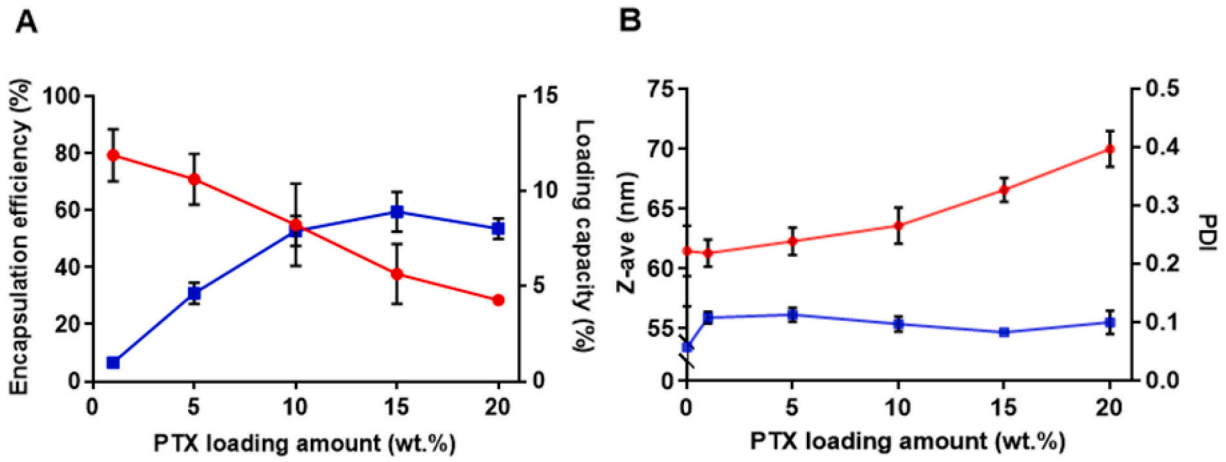

Fig. 4. (**A**) Encapsulation efficiency (red line) and loading capacity (blue line) of p(HPMAm)$_{7.1k}$-b-p(HPMAm-Bz)$_{15.0k}$ micelles at different PTX feeds. Data represent mean ± SD (n = 3). (**B**) The effect of PTX feed on the *Z*-average size (red line) and PDI (blue line) of p(HPMAm)$_{7.1k}$-b-p(HPMAm-Bz)$_{15.0k}$ micelles. Data represent mean ± SD (n = 3). (For interpretation of the references to colour in this figure legend, the reader is referred to the web version of this article.)

functionalized biotin (HDA-biotin) and NHS-activated CDTPA were synthesized as described previously [51–56], and obtained with the yield of 97 and 85%, respectively. Subsequently, biotin-CDTPA was obtained through NHS coupling of HDA-biotin with NHS-activated CDTPA with 94% yield. The ^{1}H NMR spectrum (Fig. S1) and mass spectrometric analysis (described in Section 2.2.5) demonstrate the successful synthesis of the desired CTA.

3.2. Synthesis of p(HPMAm)-b-p(HPMAm-Bz) block copolymers

The block copolymers p(HPMAm)-b-p(HPMAm-Bz) were synthesized as illustrated in Scheme 1B & C. First, HPMAm was polymerized by RAFT using either CDTPA or biotin-CDTPA as CTA and AIBN as initiator, respectively (Scheme 1B). The obtained p(HPMAm) macroCTA was subsequently extended with HPMAm-Bz (Scheme 1C). As shown in Fig. 1A, fast polymerization rates up to 8 h were observed, which slowed down after this time point likely due to loss of active thiocarbonylthio chain ends affording 'dead' polymer chains that are unable to participate in the RAFT process [63,64]. Similar pheonomenon in RAFT polymerization at high conversions was also observed in previous studies [57,65]. Fig. 1B–D show that the number average molecular weight (M_n) increased linearly with HPMAm and HPMAm-Bz conversion, which is typical for a controlled radical polymerization [66].

We aimed to synthesize p(HPMAm) macroCTA with molecular weights of 3, 5 and 7 kDa, respectively, to mimic PEG (2–5 kDa) commonly used as a stealth polymer in polymeric micelles and PEGylated liposomes [67–70]. To obtain p(HPMAm) of different molecular weights, the molar ratio of HPMAm/CDTPA/AIBN ([M]/[CTA]/[I]) in the feed was varied (180/5/1, 320/5/1 and 460/5/1). For the synthesis of biotinylated p(HPMAm), the feed molar ratio of HPMAm/biotin-CDTPA/AIBN was 460/5/1. The RAFT polymerization was terminated when the conversion was around 50% to obtain p(HPMAm) with PDI of 1.19–1.33 (entries 1–4 in Table 1). The M_n's of p(HPMAm) measured by GPC were in accordance with the theoretical values calculated from the conversion of HPMAm (entries 1–4 in Table 1), by comparing the integration areas of resonances from the vinyl protons of HPMAm at 5.30 ppm and the methine protons of HPMAm at 3.68 ppm (Fig. S2A). In a typical ^{1}H NMR spectrum of the biotinylated p(HPMAm) (Fig. S3B), besides the characteristic peaks for p(HPMAm), the resonances attributed to the biotin unit could be clearly identified (chemical shifts as described in Section 2.3.3), which demonstrates that the biotin-terminated p(HPMAm) was successfully synthesized by RAFT polymerization using a biotin-functionalized trithiocarbonate chain transfer agent.

To synthesize p(HPMAm)-b-p(HPMAm-Bz) diblock copolymers, the different p(HPMAm) macroCTAs were chain-extended with HPMAm-Bz under the same reaction conditions as for the synthesis of p(HPMAm). We aimed to synthesize block copolymers with a molecular weight below 45 kDa, which is the threshold of renal elimination for pHPMA [71]. To obtain p(HPMAm)-b-p(HPMAm-Bz) of different molecular weights, the molar ratios of HPMAm-Bz/p(HPMAm)/AIBN ([M]/[CTA]/[I]) in the feed were 250/5/1, 500/5/1 and 900/5/1. For the synthesis of the biotinylated block copolymer, the feed molar ratio of HPMAm-Bz/biotinylated p(HPMAm)/AIBN was 900/5/1. The RAFT polymerization was terminated when the conversion was around 40% with PDI of 1.36–1.55 (entries 5–14 in Table 1). The successful chain extension was demonstrated by GPC and ^{1}H NMR analysis. The obtained block copolymers showed a decreased GPC retention time compared to p(HPMAm), demonstrating an increased molecular weight (Fig. 2A–D). The GPC traces of the synthesized block copolymers exhibited slight tailing at low molecular weight and thus were relatively asymmetric, probably due to the presence of p(HPMAm) chains with a dead end. Such dead polymer chains formed during the macroCTA synthesis cannot undergo chain extension, resulting in a small amount of homopolymer in the final product (Fig. S7), which is inevitable when block copolymers are synthesized via RAFT [72]. The repeating units of both HPMAm and HPMAm-Bz in the ^{1}H NMR spectra support the composition of the formed block copolymers (Fig. S4B & 5B). The theoretical M_n's of the block copolymers calculated from the HPMAm-Bz conversion were close to the molecular weight values as determined by ^{1}H NMR analysis (entries 5–14 in Table 1), by comparing the integration areas of resonances from the methine protons of p(HPMAm-Bz) at 5.00 ppm and the methine protons of p(HPMAm) at 3.68 ppm (Fig. S4B). A typical ^{1}H NMR spectrum of the biotinylated p(HPMAm)-b-p(HPMAm-Bz) shows that in addition to the characteristic resonances for p(HPMAm) and p(HPMAm-Bz) units, some small peaks ascribed to biotin were found (Fig. S5B, chemical shifts as described in Section 2.3.3) providing evidence that the block copolymer p(HPMAm)-b-p(HPMAm-Bz) indeed contains the biotin end group. Importantly, only one peak was observed in the GPC chromatogram using UV detection (wavelength 210 nm, Fig. 2D), which points to the free biotin concentration below detection.

To obtain a fluorescently labeled block copolymer suitable for cellular uptake studies, p(HPMAm)$_{4.9k}$-b-p(HPMAm-Bz)$_{16.8k}$ with a terminal NHS ester group was synthesized and subsequently reacted with Cy3 amine fluorophore (Scheme S1). The M_n of the synthesized Cy3-labeled p(HPMAm)-b-p(HPMAm-Bz) as determined by ^{1}H NMR was 23.6 kDa, which is close to the number average of molecular weight of the copolymer before Cy3 conjugation (Fig. S6A & B). The GPC

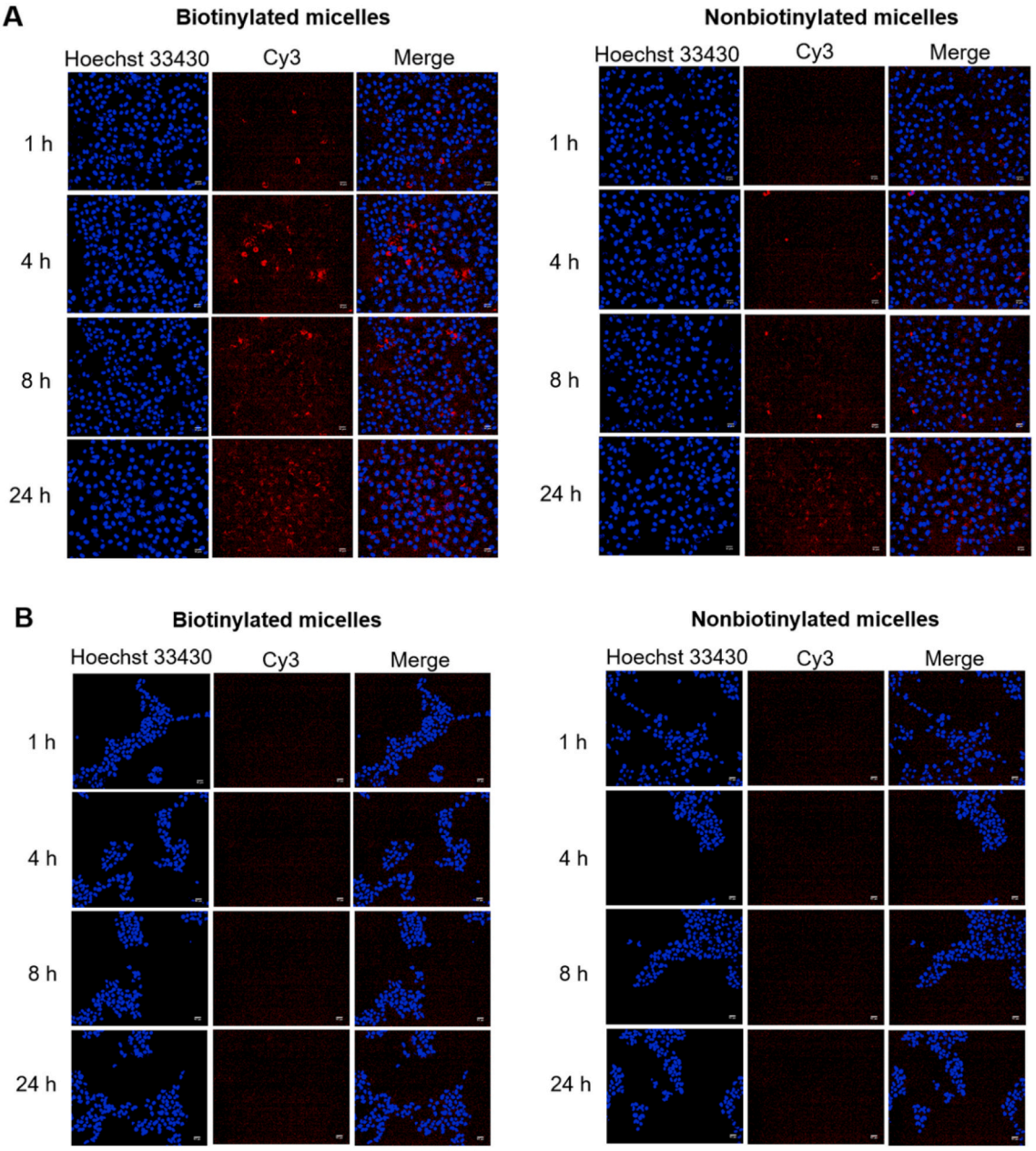

(caption on next page)

Fig. 5. Internalization of the fluorescently labeled targeted and non-targeted p(HPMAm)-b-p(HPMAm-Bz) micelles. Laser confocal scanning microscopy images of A549 cells (**A**) and HEK293 cells (**B**) after incubation with Cy3-labeled p(HPMAm)-b-p(HPMAm-Bz) micelles with or without biotin decoration (140 μg/mL) for 1, 4, 8, and 24 h. Cell nuclei are stained with Hoechst 33430 in blue while the micelles are visualized in red by Cy3. (**C**) The corresponding mean fluorescence intensity calculated from the confocal images. Scale bar = 50 μm, data represent mean ± SD (n = 5 imaging fields), * $p < 0.05$. (For interpretation of the references to colour in this figure legend, the reader is referred to the web version of this article.)

chromatogram of Cy3-labeled p(HPMAm)$_{4.9k}$-b-p(HPMAm-Bz)$_{18.7k}$ (Fig. S8A) shows that the chromatograms as recorded by RI and UV detection demonstrate identical retention time, which confirms that Cy3 was conjugated to the block copolymer. Importantly, the absence of UV–Vis signal in the Cy3-labeled p(HPMAm)$_{4.9k}$-b-p(HPMAm-Bz)$_{18.7k}$ sample at 18.5 min confirms that no free Cy3 amine was present. After the coupling reaction, on average, the number of Cy3 units was 0.85 per polymer chain as demonstrated by fluorometric analysis (Fig. S8B).

3.3. Preparation of empty p(HPMAm)-b-p(HPMAm-Bz) micelles

Polymeric micelles based on the different p(HPMAm)-b-p(HPMAm-Bz) copolymers (entries 5–13 in Table 1) were prepared by rapid addition of DMF solution containing the block copolymer to the same volume of water under stirring and followed by dialysis. ^{1}H NMR analysis showed that the residual DMF concentration was < 150 ppm, which is below the 880 ppm limit according to International Community of Harmonization (ICH) guideline for residual solvents for human use [73]. The copolymers with molecular weights ranging from 8 to 24 kDa resulted in the formation of micelles with tailored sizes from 40 to 90 nm (PDI < 0.12). As shown in Fig. 3A, for block copolymers with a fixed molecular weight of the hydrophilic p(HPMAm) block (3.0, 4.9 and 7.1 kDa), the size of the micelles increased with increasing molecular weight of hydrophobic block. This is in agreement with previous findings reported by our group, where the micelle size and aggregation number (N_{agg}) decreased with decreasing molecular weight of the hydrophobic block of the block copolymer mPEG-b-p(HPMAm-Bz) [74]. Further, the size of empty p(HPMAm)$_{7.1k}$-b-p(HPMAm-Bz)$_{15.0k}$ micelles (with or without biotin decoration) in PBS (pH 7.4) did not change upon incubation for 48 h at 37 °C (63 ± 5 and 62 ± 3 nm for biotinylated and nonbiotinylated micelles), which demonstrates good colloidal stability.

3.4. CMC of p(HPMAm)-b-p(HPMAm-Bz)

The critical micelle concentration (CMC) of the micelles based on the library of p(HPMAm)-b-p(HPMAm-Bz) block copolymers (entries 5–13 in Table 1) was determined using pyrene as a hydrophobic fluorescence probe. In the excitation spectra of pyrene, a red shift occurs as a result of pyrene partitioning from water to the hydrophobic core of polymeric micelles [75,76]. When p(HPMAm)-b-p(HPMAm-Bz) concentrations were below the CMC, a maximum peak of pyrene was observed at 333 nm, whereas this peak shifted to 338 nm when the polymer concentrations were above CMC (Fig. S9A). The I_{338}/I_{333} fluorescence ratio can thus be used to determine the CMC of polymeric micelles (Fig. S9B). The CMCs of p(HPMAm)$_{7.1k}$-b-p(HPMAm-Bz)$_{15.0k}$, p(HPMAm)$_{7.1k}$-b-p(HPMAm-Bz)$_{9.1k}$ and p(HPMAm)$_{7.1k}$-b-p(HPMAm-Bz)$_{4.9k}$ were 6, 22 and 43 μg/mL, respectively (Table 1). It is clear that for block copolymers with a fixed molecular weight of the hydrophilic block (7.1 kDa), the CMCs of the polymers decreased with increasing hydrophobic/hydrophilic ratio and thus with increasing molecular weight of the hydrophobic block. The same trend was also observed for the block polymers with fixed hydrophilic block of p(HPMAm)$_{3.0k}$ and p(HPMAm)$_{4.9k}$ (Table 1 and Fig. 3B), which is in line with previous publications [6,74,76–79].

3.5. PTX loading capacity

PTX is an antineoplastic drug and used in the treatment of various cancers [80], which is very hydrophobic and its aqueous solubility is < 0.3 μg/mL [81]. By loading this drug in p(HPMAm)$_{7.1k}$-b-p(HPMAm-Bz)$_{15.0k}$ micelles, its solubility increased to 0.5 mg/mL (Table S2). As shown in Fig. 4A, the loading capacity of p(HPMAm)$_{7.1k}$-b-p(HPMAm-Bz)$_{15.0k}$ micelles increased from 1 to 9 wt% when increasing PTX feed from 1 to 15 wt%. The loading capacity did not further increase at a 20 wt% feed of PTX, which can be attributed to the effect of the preparation methods and the solvent used in this method [77]. Our results are in accordance with previous reports showing that the introduction of benzoyl group in these micelles yielded good incorporation of hydrophobic molecules due to the π–π stacking interaction between the aromatic groups of PTX and benzoyl groups of the polymer [43,49,82]. The PTX-loaded p(HPMAm)$_{7.1k}$-b-p(HPMAm-Bz)$_{15.0k}$ micelles, dependent on the PTX content, had a slightly larger size than that of empty micelles, ranging from 61 to 70 nm with a PDI < 0.12 (Fig. 4B).

3.6. Cellular uptake of Cy3-labeled p(HPMAm)-b-p(HPMAm-Bz) micelles

Previous studies have shown that 10–20 mol% ligand (i.e., biotin and folate) density on the surface of polymeric nanoparticles was optimal for efficient cellular uptake [83,84]. We therefore fixed the biotin density at 10 mol% at the surface of the micelles. A549 (biotin receptor-positive) and HEK293 (biotin receptor-negative) cells were incubated with Cy3-labeled p(HPMAm)-b-p(HPMAm-Bz) micelles with or without biotin decoration for 1, 4, 8, and 24 h and stained with Hoechst 33430 before imaging. In non-cancerous HEK293 cells which do not express the biotin receptor, very low internalization of both biotinylated and nonbiotinylated micelles was observed (Fig. 5B & C). However, it is clear that the fluorescence intensity of biotinylated p(HPMAm)-b-p(HPMAm-Bz) micelles was significantly higher as compared to the nonbiotinylated micelles in biotin receptor-expressing A549 cells (Fig. 5A & C), confirming the enhanced internalization of biotinylated p(HPMAm)-b-p(HPMAm-Bz) micelles. Besides, the uptake of p(HPMAm)-b-p(HPMAm-Bz) micelles in these cells was time-dependent. In the presence of free biotin, biotinylated micelles showed significantly lower uptake by A549 cells whereas the uptake of nonbiotinylated micelles was not affected (Fig. S10). These observations validate that the biotinylated micelles are taken up via biotin/SMVT receptor-mediated endocytosis.

3.7. Cytotoxicity of empty and PTX-loaded p(HPMAm)-b-p(HPMAm-Bz) micelles

A549 and HEK293 cell lines were used to assess the cytocompatibility of formed micellar formulations with or without biotin modification and to determine the cytotoxicity of PTX-loaded micelles as compared to Taxol formulations. The results indicate that empty p(HPMAm)$_{7.1k}$-b-p(HPMAm-Bz)$_{15.0k}$ micelles with or without biotin modification were non-toxic at the polymer concentrations up to 1.7 mg/mL as compared to Cremophor EL/ethanol solution which showed substantial cytotoxicity above a concentration of 1.7 μg/mL (Fig. 6A & B). PTX-loaded micelles with or without biotin decoration exhibited comparable cytotoxicity for both cell lines at low PTX concentrations (up to 0.1 μg/mL) (Fig. 6C & D). This can be explained by the fact that the polymer concentration was below its CMC and thus

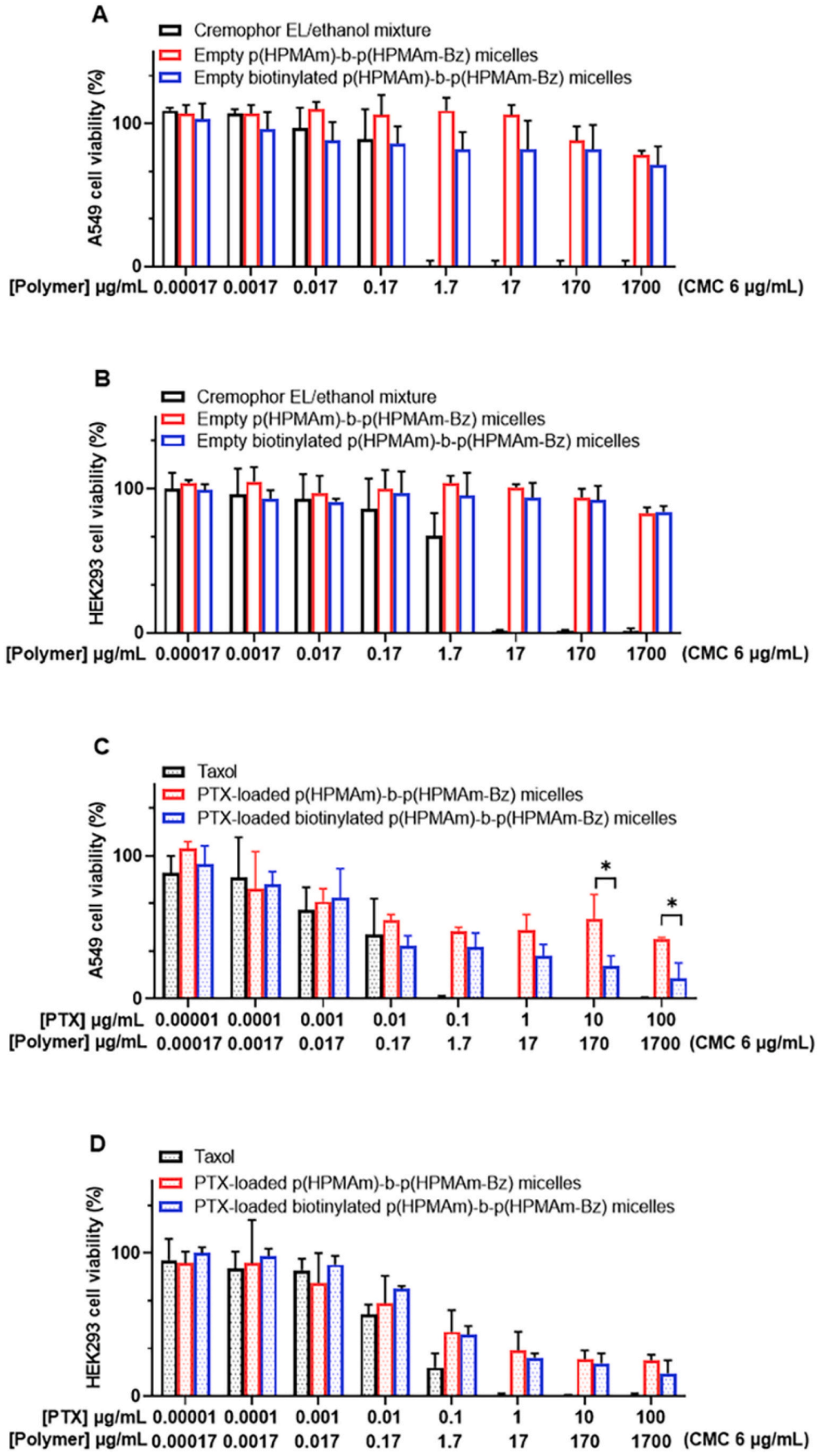

Fig. 6. Cytotoxicity of the targeted and non-targeted p(HPMAm)-b-p(HPMAm-Bz) micelles. Cell viability of A549 (**A**) and HEK293 cells (**B**) exposed to Cremophor EL/ethanol mixture and p(HPMAm)-b-p(HPMAm-Bz) micelles with or without biotin decoration. Cell viability of A549 (**C**) and HEK293 cells (**D**) exposed to Taxol and PTX-loaded p(HPMAm)-b-p(HPMAm-Bz) micelles with or without biotin decoration. Data represent mean ± SD ($n = 3$), * $p < 0.05$.

Table 2
IC_{50} values in A549 and HEK293 cells after 48 h-treatment by PTX formulations.

Cell line	IC_{50} (μg/mL)[a]		
	Taxol	PTX-loaded micelles without biotin decoration	PTX-loaded micelles with biotin decoration
A549	0.003 ± 0.001	1.5 ± 0.3	0.021 ± 0.002
HEK293	0.013 ± 0.008	0.13 ± 0.06	0.142 ± 0.015

[a] Data represent mean ± SD (n = 3).

PTX was present in its free form. At higher PTX concentrations (> 0.1 μg/mL), Taxol showed higher cytotoxicity than PTX-loaded polymeric micelles formulations due to high toxicity of Cremophor EL/ethanol mixture. Fig. 6D shows that at PTX concentration > 1 μg/mL, the cytotoxicity did not show significant difference between PTX-loaded micelles with or without biotinylation in HEK293 cells lacking the biotin receptor ($p > 0.05$). However, at PTX concentrations of 10 and 100 μg/mL, the biotinylated micelles were significantly more cytotoxic than PTX-loaded micelles without biotin modification in A549 cells which overexpress the biotin receptor ($p < 0.05$) (Fig. 6C). At PTX concentrations of 1–100 μg/mL, the polymer concentration was above CMC and therefore the significant killing enhancement of the formulation is likely caused by the released PTX after internalization of the micelles. IC_{50} values as determined using the MTS assay are summarized in Table 2, suggesting that the expression of the biotin receptor on the surface of A549 lung cancer cells induced receptor-mediated endocytosis of biotinylated micelles as compared to HEK293 cells that do not express the biotin receptor, and subsequently PTX was released from the polymeric micelles internalized by A549 cells resulting in cell killing.

4. Conclusions

In the present study, well-controlled block copolymers p(HPMAm)-b-(pHPMAm-Bz) with and without biotin functionalization were successfully synthesized by RAFT polymerization and in aqueous solution they self-assembled into polymeric micelles with tailored size above their critical micelle concentrations. The biotin-decorated micelles were more efficiently internalized and exerted more potent cytotoxicity than non-targeted micelles in target cells, which was mediated by biotin receptor expressed on the surface of the target cells. These results provide evidence that the biotinylated polymeric micelles fully based on a poly(HPMAm) backbone are promising candidates for targeted therapy of biotin receptor-overexpressing cancers.

Author contributions

Conceptualization: Y.W., Y.S., and W.E.H. Funding acquisition: Y.W. and C.F.v.N. Investigation: Y.W. and M.J.v.S. Methodology: Y.W., C.F.v.N. and W.E.H. Writing—original draft: Y.W. Writing—review and editing: N.B., Y.S., T.L., C.F.v.N. and W.E.H. Supervision: N.B., C.F.v.N. and W.E.H. All authors have read and agreed to the published version of the manuscript.

Declaration of competing interest

The authors declare no conflict of interest.

Acknowledgments

The research was partially supported by the China Scholarship Council. The authors are grateful for the technical support from Joep van den Dikkenberg.

Appendix A. Supplementary data

Supplementary data to this article can be found online at https://doi.org/10.1016/j.jconrel.2020.09.013.

References

[1] C. Deng, Y. Jiang, R. Cheng, F. Meng, Z. Zhong, Biodegradable polymeric micelles for targeted and controlled anticancer drug delivery: promises, progress and prospects, Nano Today 7 (2012) 467–480.
[2] H. Cabral, K. Kataoka, Progress of drug-loaded polymeric micelles into clinical studies, J. Control. Release 190 (2014) 465–476.
[3] A. Varela-Moreira, Y. Shi, M.H.A.M. Fens, T. Lammers, W.E. Hennink, R.M. Schiffelers, Clinical application of polymeric micelles for the treatment of cancer, Mater. Chem. Front. 1 (2017) 1485–1501.
[4] C. Allen, Why I'm holding onto hope for nano in oncology, Mol. Pharm. 13 (2016) 2603–2604.
[5] G. Gaucher, R.H. Marchessault, J.C. Leroux, Polyester-based micelles and nanoparticles for the parenteral delivery of taxanes, J. Control. Release 143 (2010) 2–12.
[6] N. Kang, J.C. Leroux, Triblock and star-block copolymers of N-(2-hydroxypropyl) methacrylamide or N-vinyl-2-pyrrolidone and d,l-lactide: synthesis and self-assembling properties in water, Polymer (Guildf) 45 (2004) 8967–8980.
[7] O. Soga, C.F. Van Nostrum, A. Ramzi, T. Visser, F. Soulimani, P.M. Frederik, P.H.H. Bomans, W.E. Hennink, Physicochemical characterization of degradable thermosensitive polymeric micelles, Langmuir 20 (2004) 9388–9395.
[8] H. Cabral, K. Miyata, K. Osada, K. Kataoka, Block copolymer micelles in nanomedicine applications, Chem. Rev. 118 (2018) 6844–6892.
[9] Y. Shi, T. Lammers, G. Storm, W.E. Hennink, Physico-chemical strategies to enhance stability and drug retention of polymeric micelles for tumor-targeted drug delivery, Macromol. Biosci. 17 (2017) e1600160.
[10] H. Maeda, H. Nakamura, J. Fang, The EPR effect for macromolecular drug delivery to solid tumors: improvement of tumor uptake, lowering of systemic toxicity, and distinct tumor imaging in vivo, Adv. Drug Deliv. Rev. 65 (2013) 71–79.
[11] H. Maeda, J. Wu, T. Sawa, Y. Matsumura, K. Hori, Tumor vascular permeability and the EPR effect in macromolecular therapeutics: a review, J. Control. Release 65 (2000) 271–284.
[12] V. Torchilin, Tumor delivery of macromolecular drugs based on the EPR effect, Adv. Drug Deliv. Rev. 63 (2011) 131–135.
[13] A. Alibakhshi, F. Abarghooi Kahaki, S. Ahangarzadeh, H. Yaghoobi, F. Yarian, R. Arezumand, J. Ranjbari, A. Mokhtarzadeh, M. de la Guardia, Targeted cancer therapy through antibody fragments-decorated nanomedicines, J. Control. Release 268 (2017) 323–334.
[14] P. Mi, H. Cabral, K. Kataoka, Ligand-installed nanocarriers toward precision therapy, Adv. Mater. 32 (2019) e1902604.
[15] V.J. Yao, S. D'Angelo, K.S. Butler, C. Theron, T.L. Smith, S. Marchiò, J.G. Gelovani, R.L. Sidman, A.S. Dobroff, C.J. Brinker, A.R.M. Bradbury, W. Arap, R. Pasqualini, Ligand-targeted theranostic nanomedicines against cancer, J. Control. Release 240 (2016) 267–286.
[16] J. Li, F. Wang, D. Sun, R. Wang, A review of the ligands and related targeting strategies for active targeting of paclitaxel to tumours, J. Drug Target 24 (2016) 590–602.
[17] Y. Lu, P.S. Low, Folate-mediated delivery of macromolecular anticancer therapeutic agents, Adv. Drug Deliv. Rev. 54 (2002) 675–693.
[18] R. van der Meel, L.J.C. Vehmeijer, R.J. Kok, G. Storm, E.V.B. van Gaal, Ligand-targeted particulate nanomedicines undergoing clinical evaluation: current status, Adv. Drug Deliv. Rev. 65 (2013) 1284–1298.
[19] W. Alshaer, H. Hillaireau, E. Fattal, Aptamer-guided nanomedicines for anticancer drug delivery, Adv. Drug Deliv. Rev. 134 (2018) 122–137.
[20] W.X. Ren, J. Han, S. Uhm, Y.J. Jang, C. Kang, J.S.H. Kim, J.S.H. Kim, Recent development of biotin conjugation in biological imaging, sensing, and target delivery, Chem. Commun. 51 (2015) 10403–10418.
[21] S. Chen, X. Zhao, J. Chen, J. Chen, L. Kuznetsova, S.S. Wong, I. Ojima, Mechanism-based tumor-targeting drug delivery system. validation of efficient vitamin receptor-mediated endocytosis and drug release, Bioconjug. Chem. 21 (2010) 979–987.
[22] S.W. Polyak, Mechanisms of biotin transport, Biochem. Anal. Biochem. 4 (2015) 1–8.
[23] G. Russell-Jones, K. McTavish, J. McEwan, J. Rice, D. Nowotnik, Vitamin-mediated targeting as a potential mechanism to increase drug uptake by tumours, J. Inorg. Biochem. 98 (2004) 1625–1633.
[24] G. Russell-Jones, J. Mcewan, Amplification of biotin-mediated targeting, US patent 2006/0127310 A1, application no. 10/535, 269, Access Pharmaceuticals Australia PTY LTD., USA, 2006.
[25] N.U. Deshpande, M. Jayakannan, Biotin-tagged polysaccharide vesicular nanocarriers for receptor-mediated anticancer drug delivery in cancer cells, Biomacromolecules 19 (2018) 3572–3585.
[26] H. Nosrati, P. Barzegari, H. Danafar, H. Kheiri, F. Group, Biotin-functionalized copolymeric PEG-PCL micelles for in vivo tumour-targeted delivery of artemisinin, Artif. Cells, Nanomedi. Biotechnol. 47 (2019) 104–114.
[27] C.Y. Deng, Y.Y. Long, S. Liu, Z.B. Chen, C. Li, Construction of biotin-modified polymeric micelles for pancreatic cancer targeted photodynamic therapy, Yaoxue Xuebao 50 (2015) 1038–1044.
[28] E.Y. Hanurry, T.W. Mekonnen, A.T. Andrgie, H.F. Darge, Y.S. Birhan, W.-H. Hsu, H.-Y. Chou, C.-C. Cheng, J.-Y. Lai, H.-C. Tsai, Biotin-decorated PAMAM G4.5

dendrimer nanoparticles to enhance the delivery, anti-proliferative, and apoptotic effects of chemotherapeutic drug in cancer cells, Pharmaceutics 12 (2020) e443.
[29] Y. Jin, Z. Wu, C. Wu, Y. Zi, X. Chu, J. Liu, W. Zhang, Size-adaptable and ligand (biotin)-sheddable nanocarriers equipped with avidin scavenging technology for deep tumor penetration and reduced toxicity, J. Control. Release 320 (2020) 142–158.
[30] S. Maiti, P. Paira, Biotin conjugated organic molecules and proteins for cancer therapy: a review, Eur. J. Med. Chem. 145 (2018) 206–223.
[31] R. Narain, M. Gonzales, A.S. Hoffman, P.S. Stayton, K.M. Krishnan, Synthesis of monodisperse biotinylated p(NIPAAm)-coated iron oxide magnetic nanoparticles and their bioconjugation to streptavidin, Langmuir 23 (2007) 6299–6304.
[32] A. Aqil, H. Qiu, J.F. Greisch, R. Jérôme, E. De Pauw, C. Jérôme, Coating of gold nanoparticles by thermosensitive poly(N-isopropylacrylamide) end-capped by biotin, Polymer (Guildf) 49 (2008) 1145–1153.
[33] C.Y. Hong, C.Y. Pan, Direct synthesis of biotinylated stimuli-responsive polymer and diblock copolymer by RAFT polymerization using biotinylated trithiocarbonate as RAFT agent, Macromolecules 39 (2006) 3517–3524.
[34] A. Doerflinger, N.N. Quang, E. Gravel, G. Pinna, M. Vandamme, F. Ducongé, E. Doris, Biotin-functionalized targeted polydiacetylene micelles, Chem. Commun. 54 (2018) 3613–3616.
[35] W. Lv, L. Liu, Y. Luo, X. Wang, Y. Liu, Biotinylated thermoresponsive core cross-linked nanoparticles via RAFT polymerization and “click” chemistry, J. Colloid Interface Sci. 356 (2011) 16–23.
[36] K. Knop, R. Hoogenboom, D. Fischer, U.S. Schubert, Poly(ethylene glycol) in drug delivery: pros and cons as well as potential alternatives, Angew. Chem. Int. Ed. 49 (2010) 6288–6308.
[37] I. Alberg, S. Kramer, M. Schinnerer, Q. Hu, C. Seidl, C. Leps, N. Drude, D. Möckel, C. Rijcken, T. Lammers, M. Diken, M. Maskos, S. Morsbach, K. Landfester, S. Tenzer, M. Barz, R. Zentel, Polymeric nanoparticles with neglectable protein corona, Small (2020) e1907574.
[38] L. Houdaihed, J.C. Evans, C. Allen, Overcoming the road blocks: advancement of block copolymer micelles for cancer therapy in the clinic, Mol. Pharm. 14 (2017) 2503–2517.
[39] Z.R. Lu, P. Qiao, Drug delivery in cancer therapy, quo vadis? Mol. Pharm. 15 (2018) 3603–3616.
[40] E.T.M. Dams, P. Laverman, W.J.G. Oyen, G. Storm, G.L. Scherphof, J.W.M. van der Meer, F.H.M. Corstens, O.C. Boerman, Accelerated blood clearance and altered biodistribution of repeated injections of sterically stabilized liposomes, J. Pharmacol. Exp. Ther. 292 (2000) 1071–1079.
[41] A.S. Abu Lila, H. Kiwada, T. Ishida, The accelerated blood clearance (ABC) phenomenon: clinical challenge and approaches to manage, J. Control. Release 172 (2013) 38–47.
[42] M. Talelli, C.J.F. Rijcken, C.F. van Nostrum, G. Storm, W.E. Hennink, Micelles based on HPMA copolymers, Adv. Drug Deliv. Rev. 62 (2010) 231–239.
[43] Y. Shi, M.J. Van Steenbergen, E.A. Teunissen, L. Novo, S. Gradmann, M. Baldus, C.F. Van Nostrum, W.E. Hennink, Π-Π stacking increases the stability and loading capacity of thermosensitive polymeric micelles for chemotherapeutic drugs, Biomacromolecules 14 (2013) 1826–1837.
[44] T. Minko, P. Kopečková, V. Pozharov, J. Kopeček, HPMA copolymer bound adriamycin overcomes MDR1 gene encoded resistance in a human ovarian carcinoma cell line, J. Control. Release 54 (1998) 223–233.
[45] J. Yang, J. Kopeček, Design of smart HPMA copolymer-based nanomedicines, J. Control. Release 240 (2016) 9–23.
[46] J. Kopeček, P. Kopečková, HPMA copolymers: origins, early developments, present, and future, Adv. Drug Deliv. Rev. 62 (2010) 122–149.
[47] J. Yang, J. Kopeček, The light at the end of the tunnel—second generation HPMA conjugates for cancer treatment, Curr. Opin. Colloid Interface Sci. 31 (2017) 30–42.
[48] P.H. Kierstead, H. Okochi, V.J. Venditto, T.C. Chuong, S. Kivimae, J.M.J. Fréchet, F.C. Szoka, The effect of polymer backbone chemistry on the induction of the accelerated blood clearance in polymer modified liposomes, J. Control. Release 213 (2015) 1–9.
[49] Y. Shi, R. Van Der Meel, B. Theek, E. Oude Blenke, E.H.E. Pieters, M.H.A.M. Fens, J. Ehling, R.M. Schiffelers, G. Storm, C.F. Van Nostrum, T. Lammers, W.E. Hennink, Complete regression of xenograft tumors upon targeted delivery of paclitaxel via Π-Π stacking stabilized polymeric micelles, ACS Nano 9 (2015) 3740–3752.
[50] D. Oupický, Č. Koňák, K. Ulbrich, DNA complexes with block and graft copolymers of N-(2-hydroxypropyl)methacrylamide and 2-(trimethylammonio)ethyl methacrylate, J. Biomater. Sci. Polym. Ed. 10 (1999) 573–590.
[51] J. Buller, A. Laschewsky, J.F. Lutz, E. Wischerhoff, Tuning the lower critical solution temperature of thermoresponsive polymers by biospecific recognition, Polym. Chem. 2 (2011) 1486–1489.
[52] D. Tong, J. Yao, H. Li, S. Han, Synthesis and characterization of thermo- and pH-sensitive block copolymers bearing a biotin group at the poly(ethylene oxide) chain end, J. Appl. Polym. Sci. 102 (2006) 3552–3558.
[53] G. Miglietta, S. Cogoi, J. Marinello, G. Capranico, A.S. Tikhomirov, A. Shchekotikhin, L.E. Xodo, RNA G-quadruplexes in kirsten ras (KRAS) oncogene as targets for small molecules inhibiting translation, J. Med. Chem. 60 (2017) 9448–9461.
[54] J. Brglez, I. Ahmed, C.M. Niemeyer, Photocleavable ligands for protein decoration of DNA nanostructures, Org. Biomol. Chem. 13 (2015) 5102–5104.
[55] O.O. Oyeneye, W.Z. Xu, P.A. Charpentier, Adhesive RAFT agents for controlled polymerization of acrylamide: effect of catechol-end R groups, RSC Adv. 5 (2015) 76919–76926.
[56] D.S.W. Benoit, S. Srinivasan, A.D. Shubin, P.S. Stayton, Synthesis of folate-functionalized RAFT polymers for targeted siRNA delivery, Biomacromolecules 12 (2011) 2708–2714.
[57] Y. Shi, E.T.A. Van Den Dungen, B. Klumperman, C.F. Van Nostrum, W.E. Hennink, Reversible addition-fragmentation chain transfer synthesis of a micelle-forming, structure reversible thermosensitive diblock copolymer based on the N-(2-hydroxy propyl) methacrylamide backbone, ACS Macro Lett. 2 (2013) 403–408.
[58] M. Najafi, N. Kordalivand, M.A. Moradi, J. Van Den Dikkenberg, R. Fokkink, H. Friedrich, N.A.J.M. Sommerdijk, M. Hembury, T. Vermonden, Native chemical ligation for cross-linking of flower-like micelles, Biomacromolecules 19 (2018) 3766–3775.
[59] A. Swami, M.R. Reagan, P. Basto, Y. Mishima, N. Kamaly, S. Glavey, S. Zhang, M. Moschetta, D. Seevaratnam, Y. Zhang, J. Liu, M. Memarzadeh, J. Wu, S. Manier, J. Shi, N. Bertrand, Z.N. Lu, K. Nagano, R. Baron, A. Sacco, A.M. Roccaro, O.C. Farokhzad, I.M. Ghobrial, Engineered nanomedicine for myeloma and bone microenvironment targeting, Proc. Natl. Acad. Sci. U. S. A. 111 (2014) 10287–10292.
[60] O. Naksuriya, Y. Shi, C.F. Van Nostrum, S. Anuchapreeda, W.E. Hennink, S. Okonogi, HPMA-based polymeric micelles for curcumin solubilization and inhibition of cancer cell growth, Eur. J. Pharm. Biopharm. 94 (2015) 501–512.
[61] C. Cheng, H. Wei, J.L. Zhu, C. Chang, H. Cheng, C. Li, S.X. Cheng, X.Z. Zhang, R.X. Zhuo, Functionalized thermoresponsive micelles self-assembled from biotin-PEG-b-P(NIPAAm-co-HMAAm)-b-PMMA for tumor cell target, Bioconjug. Chem. 19 (2008) 1194–1201.
[62] J.A. Barltrop, T.C. Owen, A.H. Cory, J.G. Cory, 5-(3-carboxymethoxyphenyl)-2-(4,5-dimethylthiazolyl)-3-(4-sulfophenyl)te trazolium, inner salt (MTS) and related analogs of 3-(4,5-dimethylthiazolyl)-2,5-diphenyltetrazolium bromide (MTT) reducing to purple water-soluble formazans as cell-viability indica, Bioorg. Med. Chem. Lett. 1 (1991) 611–614.
[63] X. Pan, F. Zhang, B. Choi, Y. Luo, X. Guo, A. Feng, S.H. Thang, Effect of solvents on the RAFT polymerization of N-(2-hydroxypropyl) methacrylamide, Eur. Polym. J. 115 (2019) 166–172.
[64] B.A. Abel, C.L. McCormick, Mechanistic insights into temperature-dependent trithiocarbonate chain-end degradation during the RAFT polymerization of N-arylmethacrylamides, Macromolecules 49 (2016) 465–474.
[65] M. Danial, S. Telwatte, D. Tyssen, A. Postma, S. Cosson, G. Tachedjian, G. Moad, A. Postma, Combination anti-HIV therapy: via tandem release of prodrugs from macromolecular carriers, Polym. Chem. 7 (2016) 7477–7487.
[66] W.A. Braunecker, K. Matyjaszewski, Controlled/living radical polymerization: features, developments, and perspectives, Prog. Polym. Sci. 32 (2007) 93–146.
[67] S. Eetezadi, S.N. Ekdawi, C. Allen, The challenges facing block copolymer micelles for cancer therapy: in vivo barriers and clinical translation, Adv. Drug Deliv. Rev. 91 (2015) 7–22.
[68] Z. Amoozgar, Y. Yeo, Recent advances in stealth coating of nanoparticle drug delivery systems, Wiley Interdiscip. Rev. Nanomed. Nanobiotechnol. 4 (2012) 219–233.
[69] K. Hirota, E. Czogala, W. Pedrycz, Stealth liposomes: review of the basic science, rationale, and clinical applications, existing and potential, Int. J. Nanomedicine 1 (2016) 297–315.
[70] S. Salmaso, P. Caliceti, Stealth properties to improve therapeutic efficacy of drug nanocarriers, J. Drug Deliv. 2013 (2013) e374252.
[71] L. Seymour, R. Duncan, J. Strohalm, J. Kopeček, Effect of molecular weight (Mw) of N-(2-hydroxypropyl)methacrylamide copolymers on body distribution and rate of excretion after subcutaneous, intraperitoneal, and intravenous administration to rats, J. Biomed. Mater. Res. 21 (1987) 1341–1358.
[72] C. Barner-Kowollik, Complex architecture design via the RAFT process: scope, strengths and limitations, in: M.H. Stenzel (Ed.), Handbook of RAFT polymerization, Wiley, Sydney, 2008, pp. 315–372.
[73] International Community of Harmonization (ICH), Impurities: guideline for residual solvents Q3C (R6), Int. Conf. Harmon. Tech. Requir. Regist. Pharm. Hum. Use. 44 (2011) 1–29.
[74] M. Bagheri, J. Bresseleers, A. Varela Moreira, O. Sandre, S.A. Meeuwissen, R.M. Schiffelers, J.M. Metselaar, C.F. van Nostrum, J.C.M. van Hest, W.E. Hennink, The effect of formulation and processing parameters on the size of mPEG-b-p (HPMA-Bz) polymeric micelles, Langmuir 34 (2018) 15495–15506.
[75] C. Le Zhao, M.A. Winnik, G. Riess, M.D. Croucher, Fluorescence probe techniques used to study micelle formation in water-soluble block copolymers, Langmuir 6 (1990) 514–516.
[76] C. Kim, S.C. Lee, J.H. Shin, J.S. Yoon, I.C. Kwon, S.Y. Jeong, Amphiphilic diblock copolymers based on poly(2-ethyl-2-oxazoline) and poly(1,3-trimethylene carbonate): synthesis and micellar characteristics, Macromolecules 33 (2000) 7448–7452.
[77] Y. Hussein, M. Youssry, Polymeric micelles of biodegradable diblock copolymers: enhanced encapsulation of hydrophobic drugs, Materials (Basel) 11 (2018) e11050688.
[78] K. Letchford, R. Liggins, H. Burt, Solubilization of hydrophobic drugs by methoxy poly(ethylene glycol)-block-polycaprolactone diblock copolymer micelles: theoretical and experimental data and correlations, J. Pharm. Sci. 9 (2008) 1179–1190.
[79] K. Letchford, J. Zastre, R. Liggins, H. Burt, Synthesis and micellar characterization of short block length methoxy poly(ethylene glycol)-block-poly(caprolactone) diblock copolymers, Colloids Surf. B: Biointerfaces 35 (2004) 81–91.
[80] A.M. Barbuti, Z.S. Chen, Paclitaxel through the ages of anticancer therapy: exploring its role in chemoresistance and radiation therapy, Cancers (Basel) 7 (2015) 2360–2371.
[81] T. Konno, J. Watanabe, K. Ishihara, Enhanced solubility of paclitaxel using water-

soluble and biocompatible 2-methacryloyloxyethyl phosphorylcholine polymers, J. Biomed. Mater. Res. - Part A 65 (2003) 209–214.

[82] M. Sheybanifard, N. Beztsinna, M. Bagheri, E.M. Buhl, J. Bresseleers, A. Varela-Moreira, Y. Shi, C.F. van Nostrum, G. van der Pluijm, G. Storm, W.E. Hennink, T. Lammers, J.M. Metselaar, Systematic evaluation of design features enables efficient selection of Π electron-stabilized polymeric micelles, Int. J. Pharm. 584 (2020) e119409.

[83] N. MacKiewicz, J. Nicolas, N. Handké, M. Noiray, J. Mougin, C. Daveu, H.R. Lakkireddy, D. Bazile, P. Couvreur, Precise engineering of multifunctional PEGylated polyester nanoparticles for cancer cell targeting and imaging, Chem. Mater. 26 (2014) 1834–1847.

[84] Y.C. Gong, X.Y. Xiong, X.J. Ge, Z.L. Li, Y.P. Li, Effect of the folate ligand density on the targeting property of folated-conjugated polymeric nanoparticles, Macromol. Biosci. 19 (2019) e1800348.